ABSTRACT

Title of thesis: DESIGN AND SIMULATION OF SINE-GORDON LATTICE SYSTEM

Miao Zhang, Master of Science, 2015

Thesis directed by: Professor Robert Newcomb
Department of Electrical and Computer Engineering

The sine-Gordon equation is one of the nonlinear and integrable partial differential equations that can be solved exactly and has soliton solution. This equation was first introduced for Josephson junction propagation and has been applied to many other scientific fields.

Based on three discretized forms of the sine-Gordon equation, i.e. conventional discrete sine-Gordon equation, Orfanidis's discrete sine-Gordon equation and sine-lattice equation, we create and simulate three sine-Gordon lattice systems. By taking the difference between the adjacent outputs as the transmitting soliton signal, it is shown that all three systems could propagate the bell-shaped signal constantly and the sine-lattice equation system gives the best results.

Due to the low-voltage, low-power feature, we choose the MOS translinear circuit that exploits bulk voltages under weak inversion to realize the sine function in the sine-Gordon lattice system and the complete circuit of the sine-Gordon cell is also created utilizing this MOS translinear sin(x) circuit.

DESIGN AND SIMULATION OF SINE-GORDON LATTICE SYSTEM

by

Miao Zhang

Thesis submitted to the Faculty of the Graduate School of the
University of Maryland, College Park in partial fulfillment
of the requirements for the degree of
Master of Science
2015

Advisory Committee:

Professor Robert Newcomb, Chair
Professor Agis Iliadis
Professor Yavuz Oruc

Acknowledgements

First, I would like to thank my advisor, Professor Robert Newcomb, for providing me with the guidance and resources necessary to produce this work. Next, I would like to thank the members of my thesis defense committee, Professor Yavuz Oruc, and Professor Agis Iliadis. I would also like to thank my academic advisor, Professor Thomas Murphy. Thanks also go to Melanie Prange and Bill Churma for providing administrative support. I must also thank my parents, Junling Ma, and Jie Zhang, for making all things possible for me. Thanks also go to Yang Xie for providing encouragement for many years. I also thank Xin Xu and Yitian Wang for always lending a helpful hand and a kind ear. Furthermore, I would like to thank many of my other friends and colleagues, too numerous to name, for the many joyous times.

Table of Contents

List of Figures

Chapter 1 Introduction

1.1 Soliton and Sine-Gordon Equation

Solitons are solitary waves that preserve their shape while propagating constantly due to the cancellation of the combination of nonlinear and dispersive effects; they can emerge from an interaction without change in their shapes. They were first discovered in shallow water waves by Scott-Russell in 1834 [1] and in 1895 Korteweg and deVries [2] provided an equation for this kind of wave. Solitons can also occur in optic systems, biology systems and magnetic systems. They are the solutions of a class of nonlinear dispersive partial differential equations that describe the above physical systems, beside the Kortewege-de Vries equation, there are many more such as the Toda lattice and other nonlinear lattice equations, the self-introduced transparency equation, the sine-Gordon equation, the Boussinesq equation, the nonlinear Schrodinger equation, the Hirota equation, and the Born-Infreld equation [3].

The sine-Gordon equation is the one of interest here. It is a nonlinear hyperbolic partial differential equation. There are two main forms of this equation. The one in the space-time coordinates is given by (1.1)

$$\varphi_{tt} - \varphi_{xx} + \sin\varphi = 0$$

and the one in the light cone coordinates is given by

$$\varphi_{uv} = \sin\varphi \tag{1.2}$$

where

$$u = \frac{x+t}{2}, \text{ and } v = \frac{x-t}{2} \tag{1.3}$$

A more general form of the sine-Gordon equation is

$$\varphi_{tt} - \varphi_{xx} + m^2 \sin\varphi = 0 \tag{1.4}$$

The sine-Gordon equation is integrable and can be solved exactly. The solutions of the sine-Gordon equation are solitons, kinks and breathers, which are one-soliton solutions, two-soliton solutions that describe the kink-kink or kink-antikink collisions, and other two-soliton solutions that describe the oscillatory behavior of coupled kink and antikink, respectively. They appear in the propagations of magnetic flux in long Josephson junctions, dislocations in crystals, intra-cellular and inter-cellular dynamics in living cellular structures, and many other situations [4]. The soliton solutions of the sine-Gordon equation attract most attention and the 1-soliton solutions of equation (1.3) is

$$\varphi(x,t) = 4\tan^{-1}(e^{\frac{m(x-vt)}{1-v^2}+\delta}) \tag{1.5}$$

where v is the velocity of propagation and m and δ are other constants. By discretizing the sine-Gordon equation, a discrete lattice system that transmits solitons can be constructed as show in chapter 2. The basic blocks of the cell, which is cascaded in the lattice system, are merely adders, subtractors, integrators, amplifiers and sine functions. All of these building blocks can be realized by bipolar or MOS transistor circuits. However, the sine circuits are less common and need more discussion. The circuit of the sine-Gordon lattice system can be applied to many scientific areas due to their soliton transmitting signals. For example, since the neural impulses in living cellular structures are solitions, a sine-Gordon lattice circuit can be utilized to propagate the signals in neural networks. It can also be applied to the computers that use solitons as the transmission signals.

1.2 Contributions

The contribution of this thesis can be broken into two parts: the system equation and their circuit realization.

1.1.1 Simulations of sine-Gordon lattice system

The contributions of this part are: first, we create the nth cell in a sine-Gordon lattice system using three different discrete forms of sine-Gordon equation, namely, the conventional discrete sine-Gordon equation, Orfanidis's discrete sine-Gordon equation and a sine-lattice equation; second, we construct and simulate in Simulink the 48-, 45-, and 72-cell sine-Gordon lattice systems using the three different kinds of cells respectively; third, we find that by taking the difference between the adjacent outputs as the transmitting signal, all three systems can propagate the bell-shaped signal constantly with simulation results close to theoretical values. The third system gives the best results. And therefore, we prefer to use the sine-lattice equation to construct the sine-Gordon lattice system. Since the basic cell of sine-lattice equation system contains three sine functions, we create other cell for this system that contains only two sine functions in each cell.

1.1.2 Creation of Sine-Gordon Lattice Circuit

The main contribution of this part is that we verify two MOS translinear sin(x)-circuits in Mulder's paper [5] by simulating them using mnmosis nMOS model in PSpice and then create the circuits for the cells of sine-Gordon lattice system using the sin(x)-circuits above.

1.3 Overview

This thesis is organized as follows. In this chapter, a brief introduction of solitons and the sine-Gordon equation and the contributions of this thesis have been given. In the next chapter, three sine-Gordon discrete equations, namely conventional discrete sine-Gordon equation, Orfanidis's discrete sine-Gordon equation, and sine-lattice equation, are introduced and their corresponding lattice systems are created and simulated in Matlab Simulink. In chapter 3, first, a brief review of translinear circuits and sine circuits is given with some simple examples. Next, the MOS translinear sin(x)-circuits in Mulder's paper [5] using subthreshold with back gate operation are discussed and simulated. Then the complete circuit of the sine-Gordon cell is created using the MOS translinear sin(x)-circuit mentioned above. The last chapter is devoted to concluding remarks and open problems.

Chapter 2 Simulations of Sine-Gordon Lattice System

The sine-Gordon equation is one of the nonlinear and integrable partial differential equations that can be solved exactly and has the particle-like waves, solitons, and the breather as solutions [4]. This equation was first introduced for Josephson junction propagation and often served as a prototype for 2-D nonlinear field theory. And, therefore, it has been applied to solid-state physics, nonlinear optics, differential geometry and many other scientific fields [6]. The sine-Gordon equation is given by

$$\frac{\partial^2 u}{\partial x^2} - \frac{\partial^2 u}{\partial t^2} = \sin u \tag{2.1}$$

The discrete form of the sine-Gordon equation can be used to construct the discrete lattice system that is able to yield single, moving solitons. In this chapter, we will discuss three discretization methods of the sine-Gordon equation and utilize the three discrete equations to simulate the sine-Gordon lattice system that can transmit the solitary waves.

2.1 Conventional Discrete Sine-Gordon Equation

In this part we will use the conventional discrete sine-Gordon equation

$$\frac{\mathrm{d}^2 u_n}{\mathrm{d}t^2} = u_{n-1} - 2u_n + u_{n+1} - \sin u_n\,, \qquad n = 0, \pm 1, \pm 2, \ldots \tag{2.2}$$

to create the n^{th} cell of the sine-Gordon lattice system. The equation of motion for the Frenkel and Kontorova model of harmonically coupled particles under an external periodic potential, is given by a sine-Gordon discrete equation [7]

$$\frac{\mathrm{d}^2 y_n}{\mathrm{d}t^2} = y_{n-1} - 2y_n + y_{n+1} - \frac{1}{d^2}\sin y_n\,, \qquad n = 0, \pm 1, \pm 2, \ldots \tag{2.3}$$

where d is the discreteness parameter and y_n is the relative displacement of particle n. This equation, (2.3), is obtained from the Lagrangian

$$L = \sum_{n=-\infty}^{\infty} \frac{y_n^2}{2} - \frac{1}{2}(y_{n+1} - y_n)^2 - \frac{1}{d^2}(1 - \cos y_n) \tag{2.4}$$

If we multiply Equation (2.3) by d^2 and let

$$\tau = \frac{t}{d}\ , and\ x_n = \frac{n}{d} \tag{2.5}$$

then we obtain the sine-Gordon equation (2.1). The single soliton solution of the sine-Gordon equation is given by [4]

$$u_n = 4\tan^{-1}(e^{\frac{n-vt}{1-v^2}}) \tag{2.6}$$

where v is the velocity of the moving soliton and $0 \leq v < 1$. The Matlab space-time evolution plot of

$$\omega_n(t) \equiv u_{n+1}(t) - u_n(t) \tag{2.7}$$

is shown in Fig. 2.1 with v=0.1. From this plot, we can see that the difference ω_n between u_n and u_{n+1} is a bell-type wave that propagates constantly forward as the lattice number increases. And therefore we prefer to use ω_n as the transmission signal in our sine-Gordon lattice system.

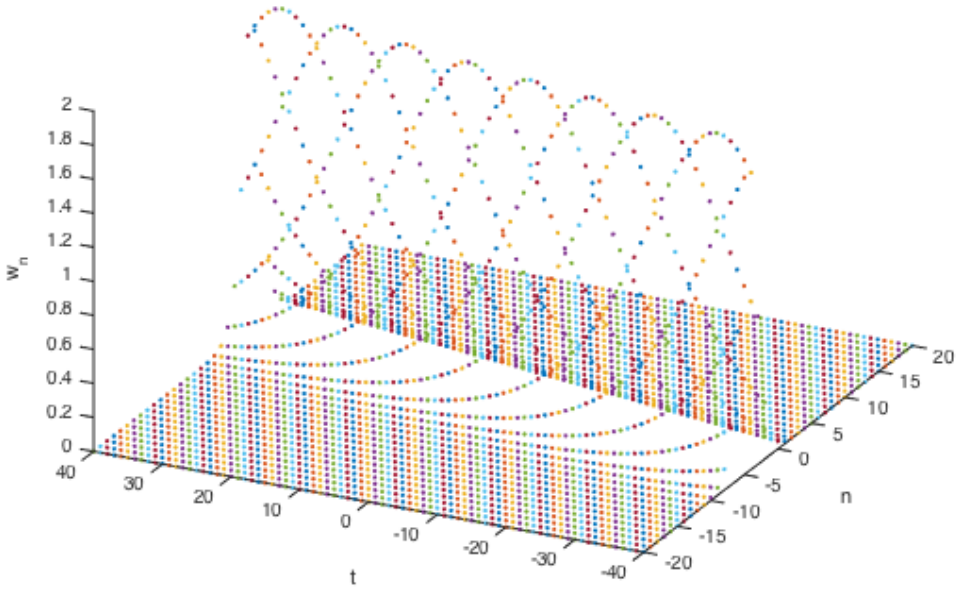

Fig. 2.1 Matlab space-time evolution plot of $\omega_n = u_{n+1} - u_n$

The Matlab Simulink model of the Equation (2.2) sine-Gordon lattice structure is shown in Fig. 2.2. There are two inputs u_{n+1} and u_{n-1}, one output u_n, one sine function and two integrators in this system. The initial conditions of the two integrators used to integrate Equation (2.2) are both zero. The amplitude and frequency of the sine function are both 1, while the bias and phase are both zero. Fig 2.3 shows how to connect the cells together. The input to the first cell is Equation (2.6) with n = 8 to represent a fully formed signal and the input In1 of the last cell is 0. The output u_n of the nth cell goes in to the $(n+1)^{th}$ cell and the $(n-1)^{th}$ cell. The inputs u_{n+1} and u_{n-1} of the nth cell are the outputs of cell n+1 and cell n-1.

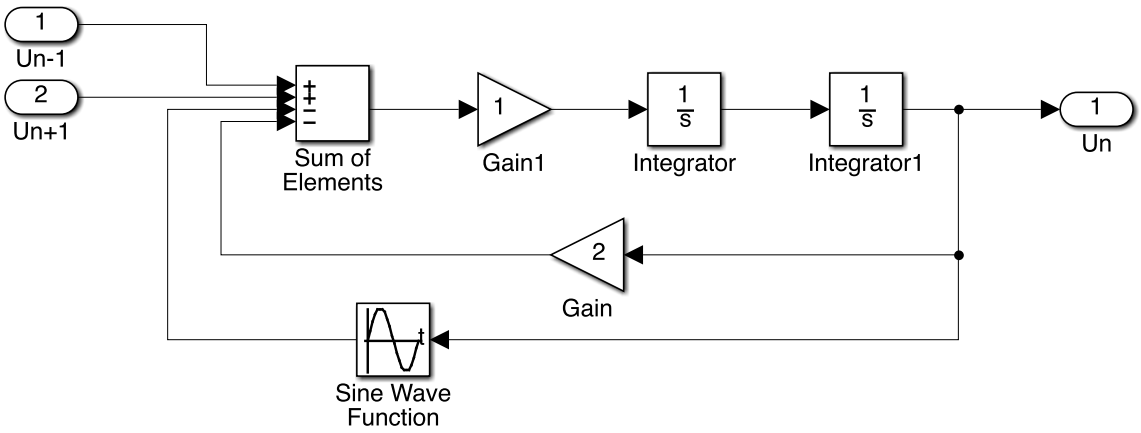

Fig. 2.2 Matlab Simulink model for the conventional discrete sine-Gordon equation (2.2)

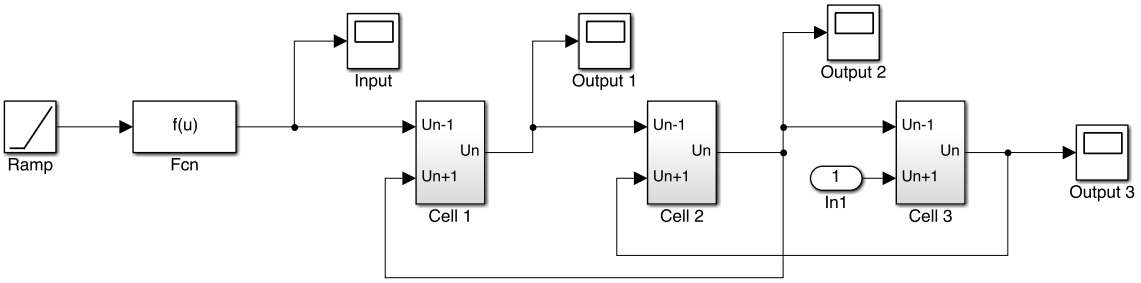

Fig. 2.3 The way to connect the conventional discrete sine-Gordon equation models

We constructed the Sine-Gordon Lattice system using 48 cells shown in Fig. 2.2 and they are connected in the way showed in Fig. 2.3. The 48-cell system using discretization of Equation (2.2) is showed in Fig. 2.4.

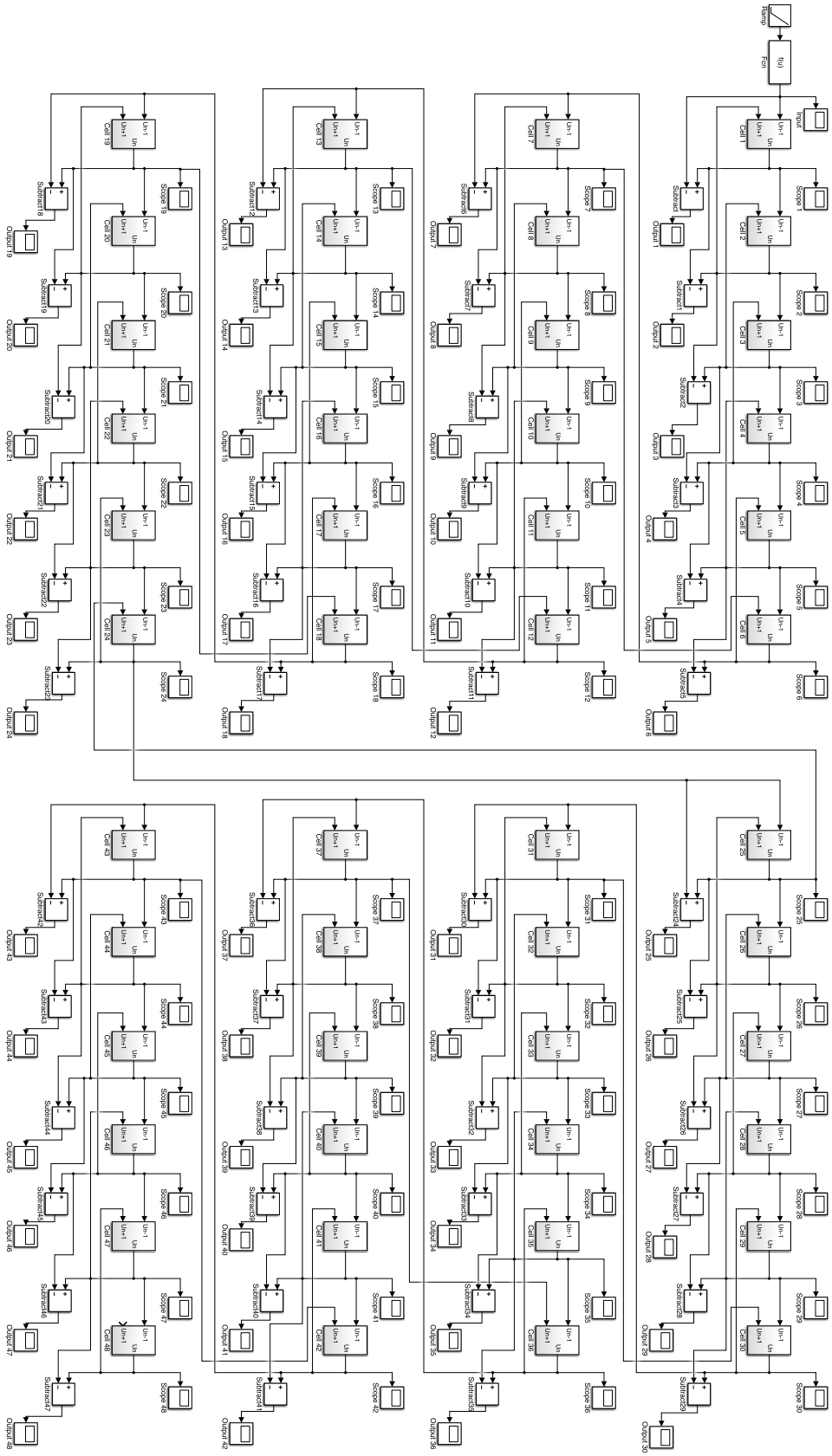

Fig. 2.4 The 48-lattice system for the conventional discrete sine-Gordon equation

From the space-time evolution plots of $\omega_n(t)$ shown in Fig. 2.1, we can conclude that instead of u_n, ω_n should be used as the transmission signal in sine-Gordon lattice system. If we take the difference of the adjacent cells u_{n+1} and u_{n-1}, and let v=0.1 and n=8, then the input of this system is

$$4\tan^{-1}(e^{\frac{8-0.1t}{0.99}}) \tag{2.8}$$

The reason that n = 8 and not 0 seems to be to set proper initial conditions on the integrators to form solutions. The plot of input signal is depicted in Fig. 2.5. The outputs u_n of the cell 1, 6, 12, 18, 24, 30, 36, 42, and 48 are shown in Fig. 2.6. From these output signals, we can see that to obtain the bell-type transmission signal, we should use the differences ω_n between the outputs of the successive cells as we discussed above.

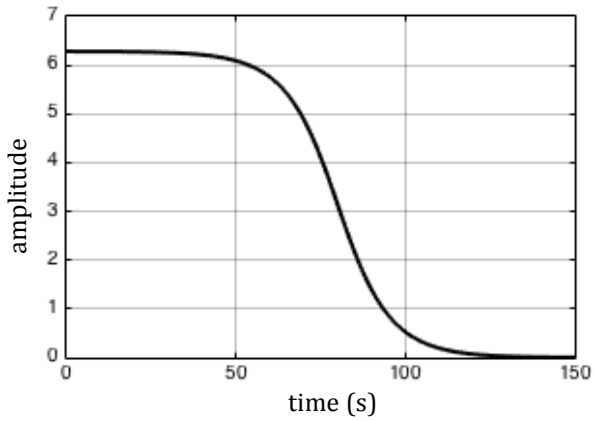

Fig. 2.5 The input of the 48-lattice system for the conventional discrete sine-Gordon equation

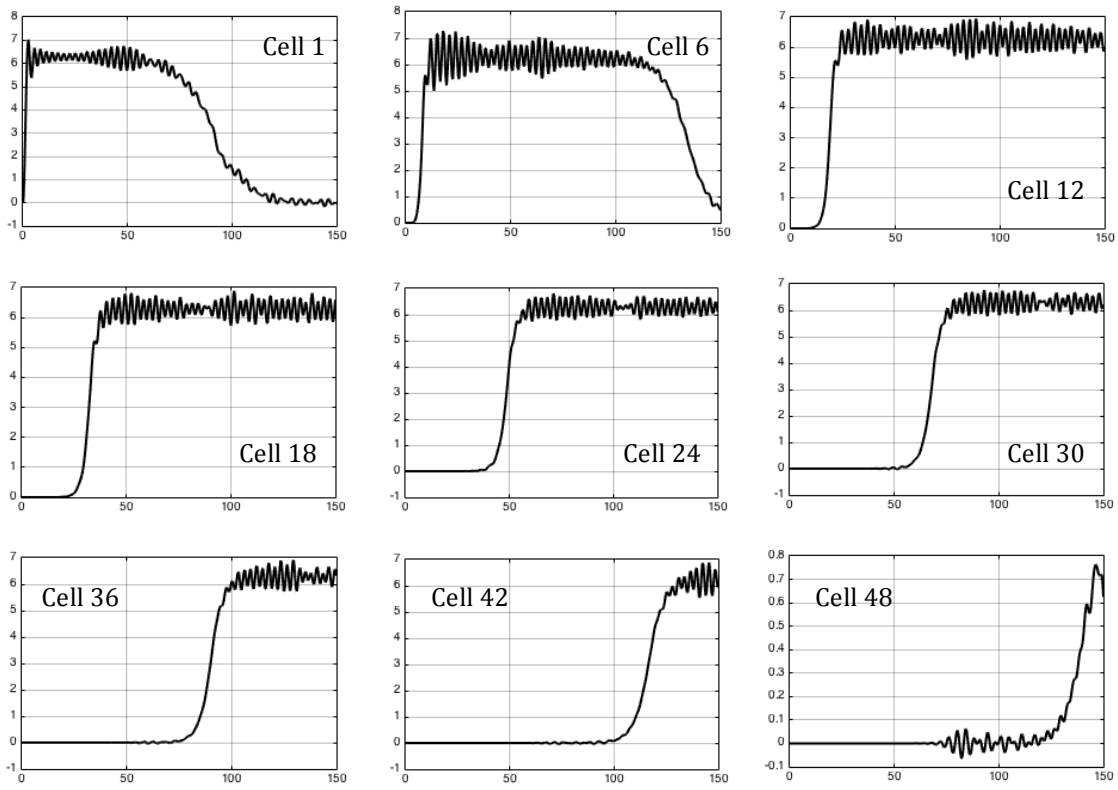

Fig. 2.6 The outputs of the cell 1, 6, 12, 18, 24, 30, 36, 42, and 48 of the 48-lattice system where the x-axes are time and y-axes are amplitude

The outputs ω_n of subtractor 1, 5, 9, 13, 17, 21, 24, 28, 32, 36, 40, and 44 are shown in Fig. 2.7 and they all contain the bell-shaped signals of similar shape and size and they are propagating constantly along the transmission path of the sine-Gordon lattice system. However, the amplitudes of these bell-shaped signals decrease while the width increases along the propagation length. Besides the changes in amplitude and shape of the bell-type signals, there is relatively large noise in this lattice system. When we simulate the sine-Gordon system with less cells, the noise signals are more significant. Therefore, one possible reason why these noise signals exist is that the number of the cells is not large enough whereas we use $n = 0, \pm 1, \pm 2, \ldots$.

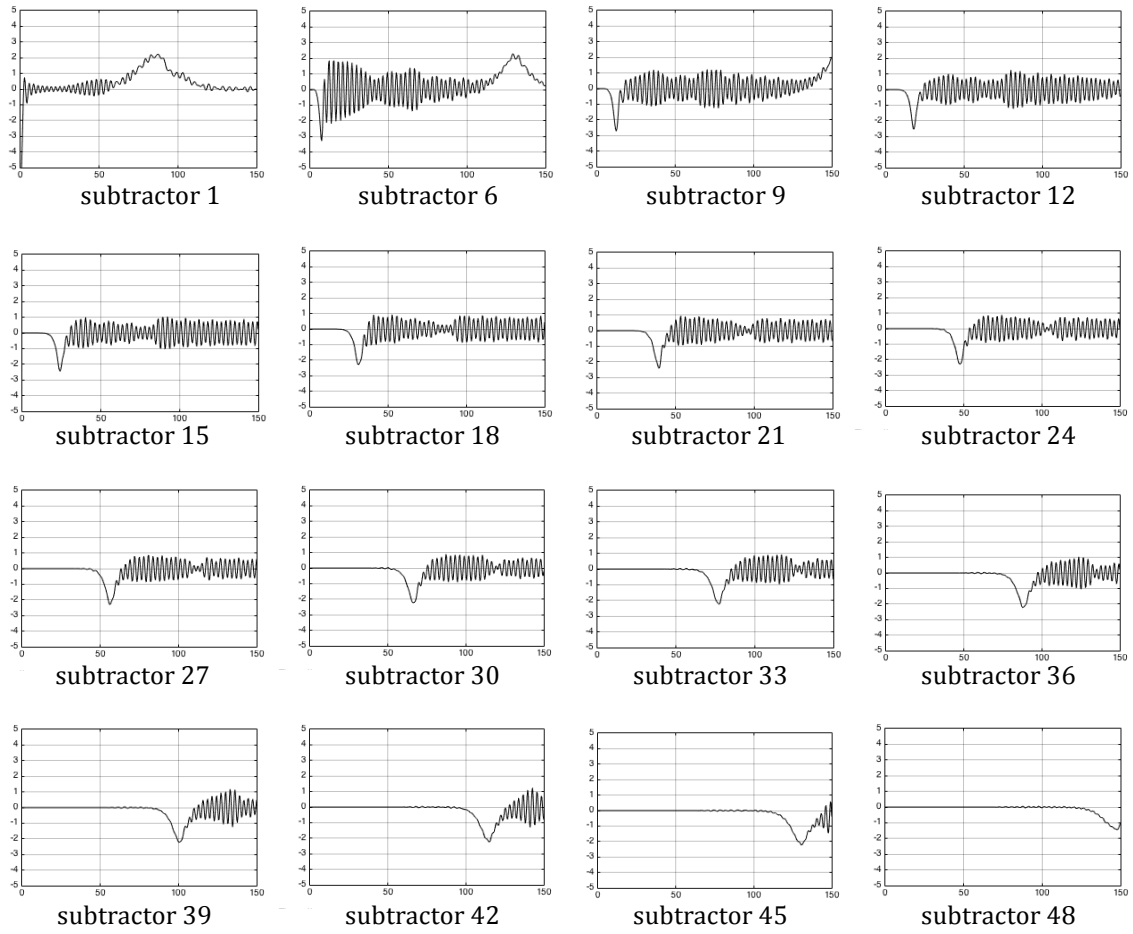

Fig. 2.7 The outputs of the subtractor 1, 6, 9, 12, 15, 18, 21, 24, 27, 30, 33, 36, 39, 42, 45, and 48 of the 48-lattice system where the x-axes are time and y-axes are amplitude

2.2 Orfanidis's Discrete Sine-Gordon Equation

In this part we will use another discrete sine-Gordon equation

$$\frac{\mathrm{d}u_{n+1}}{\mathrm{d}t} - \frac{\mathrm{d}u_n}{\mathrm{d}t} = \sin(u_{n+1} + u_n)\ , \qquad n = 0, \pm 1, \pm 2, \ldots \tag{2.9}$$

to create the cell of a sine-Gordon lattice system. This discretization was first derived by Orfanidis [8] using Hirota's method. In the space-time coordinates, the sine-Gordon equation is given by Equation (2.1')

$$\frac{\partial^2 u}{\partial x'^2} - \frac{\partial^2 u}{\partial t'^2} = \sin u \tag{2.1'}$$

while in the light-cone coordinates

$$x = \frac{x' + t'}{2}, \text{and } t = \frac{x' - t'}{2} \tag{2.10}$$

the sine-Gordon equation (2.1') becomes

$$\frac{\partial^2 u}{\partial x \partial t} = \sin u \tag{2.11}$$

if we introduce an auxiliary field $\rho(x, t)$ that satisfies

$$\frac{\partial^2 \rho}{\partial x \partial t} = 1 - \cos u \tag{2.12}$$

then we can combine Equation (2.11) and Equation (2.12) to get

$$w\frac{\partial^2 w}{\partial x \partial t} - \frac{\partial^2 w}{\partial x \partial t} = \frac{1}{4}(w^2 - w^{*2}) \tag{2.13}$$

where w is a complex variable of the form

$$w = e^{\frac{\rho + iu}{4}} \tag{2.14}$$

The space and time variables can be discretized to

$$x = nh, n = 0, \pm 1, \pm 2, \ldots, \tag{2.15a}$$

$$t = m\tau, m = 0, \pm 1, \pm 2, \ldots, \tag{2.15b}$$

where h and τ are lattice spacings. Considering the x-shift and t-shift operation, we define

$$u^x(x,t) = u(x+h,t) = u((n+1)h,t) \tag{2.16a}$$

$$u^t(x,t) = u(x,t+\tau) = u(x,(m+1)\tau) \tag{2.16b}$$

$$u^{xt}(x,t) = u(x+h,t+\tau) = u((n+1)h,(m+1)\tau) \tag{2.16c}$$

$$w^x(x,t) = w(x+h,t) = w\big((n+1)h,t\big) \tag{2.17a}$$

$$w^t(x,t) = w(x,t+\tau) = w(x,(m+1)\tau) \tag{2.17b}$$

$$w^{xt}(x,t) = w(x+h,t+\tau) = w((n+1)h,(m+1)\tau) \tag{2.17c}$$

Using Hirota's method to discretizing Equation (2.13), we get the partial difference equation

$$ww^{xt} - w^x w^t = \frac{h\tau}{4}\left(\frac{ww^{xt} + w^x w^t}{2} - \frac{w^*(w^{xt})^* - (w^x)^*(w^t)^*}{2}\right) \tag{2.18}$$

From Equation (2.14) and (2.18), the discrete sine-Gordon equation can be obtained as

$$\sin\left(\frac{u^{xt} + u - u^x - u^t}{4}\right) = \frac{h\tau}{4}\sin\left(\frac{u^{xt} + u + u^x + u^t}{4}\right) \tag{2.19}$$

In the continuous time limit $\tau \to 0$, Equation (2.19) becomes

$$\frac{\mathrm{d}u^x}{\mathrm{d}t} - \frac{\mathrm{d}u}{\mathrm{d}t} = h\sin\left(\frac{u+u^x}{2}\right) \tag{2.20}$$

If we define

$$u_{n+1} = u^x, \text{ and } u_n = u \tag{2.21}$$

then we obtain Equation (2.9).

Utilizing the hyperbolic function approach, Dai et al. [9] found some exact traveling wave solutions of Equation (2.9) and the tanh-type solutions are given by

$$u_n = 2\tan^{-1}\{\pm\tanh[kn - \frac{1}{2\tanh(k)}t + \zeta]\} \tag{2.22}$$

where k is an arbitrary constant and ζ represents a constant phase. Fig. 2.8 and 2.10 are the plots of the Equation (2.22) when k=2 and ζ=0.3. The Matlab space-time evolution plots of

$$\omega_n(t) \equiv u_{n+1}(t) - u_n(t) \tag{2.23}$$

are shown in Fig. 2.9 and Fig. 2.11. From these plot, we can see that the difference ω_n between u_n and u_{n+1} is a bell-type function and we see why we might use ω_n to transmit the signal in this sine-Gordon lattice system.

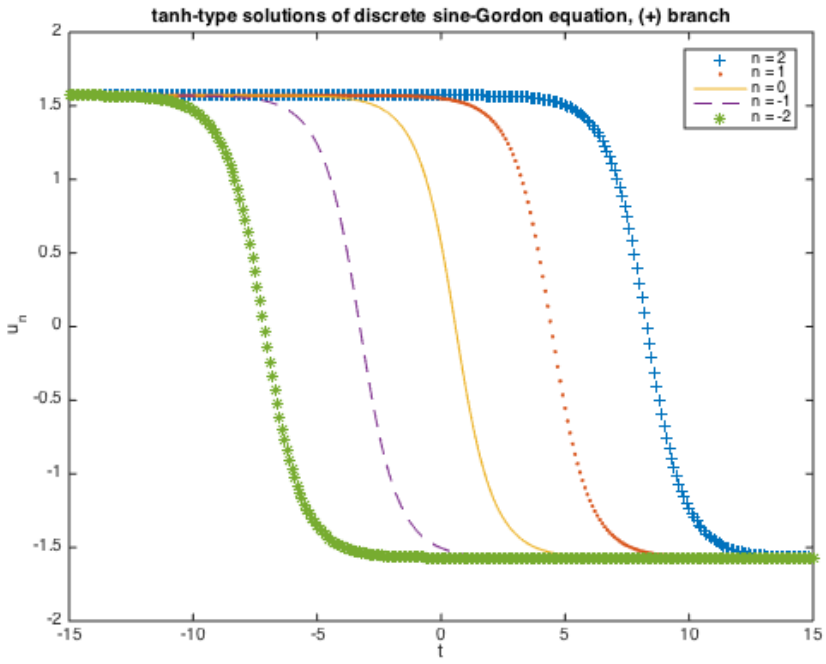

Fig. 2.8 Matlab plot of $u_n = 2\tan^{-1}\{\tanh[2n - \frac{t}{2\tanh(2)} + 0.3]\}$

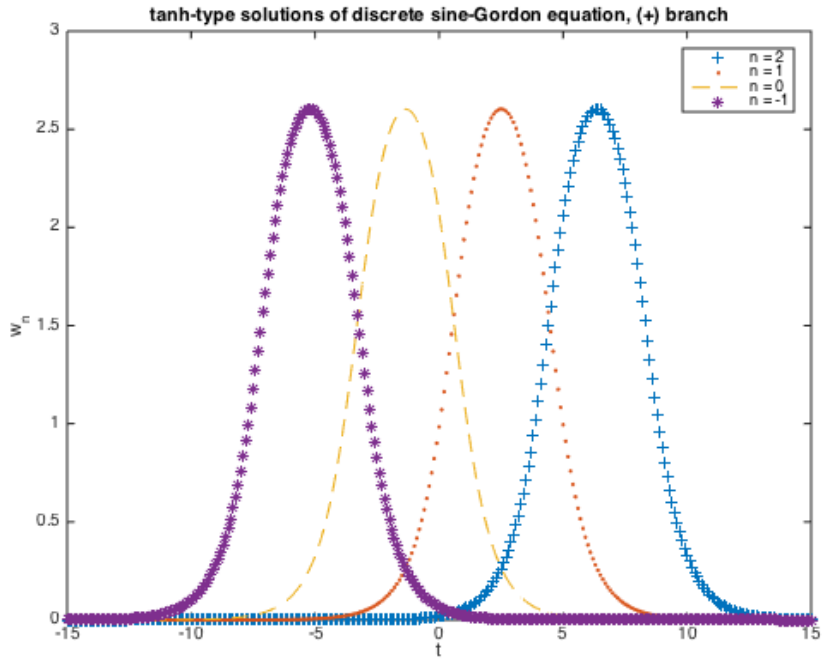

Fig. 2.9 Matlab plot of $\omega_n = u_{n+1} - u_n$ where $u_n = 2\tan^{-1}\{\tanh[2n - \frac{t}{2\tanh(2)} + 0.3]\}$

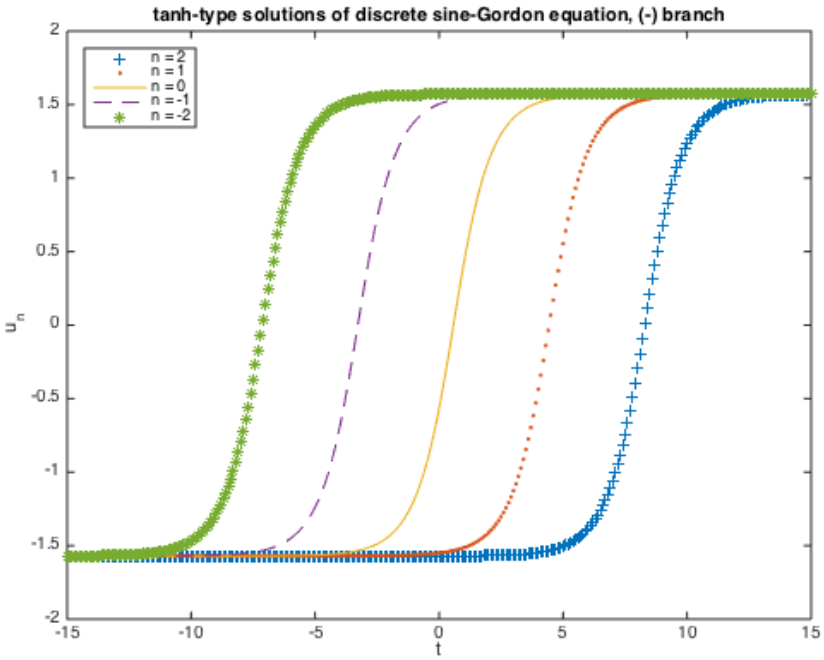

Fig. 2.10 Matlab plot of $u_n = 2\tan^{-1}\{\tanh[-2n - \frac{t}{2\tanh(2)} + 0.3]\}$

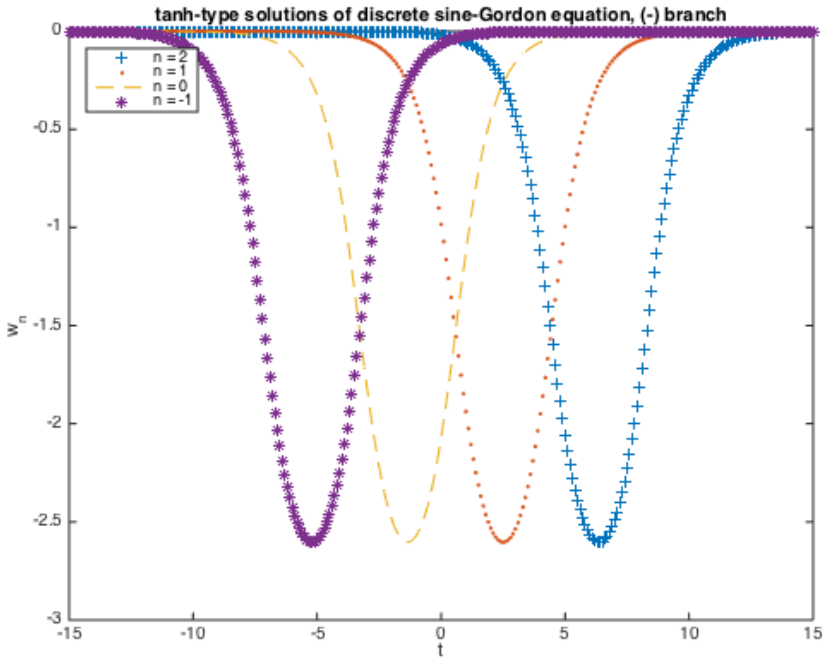

Fig. 2.11 Matlab plot of $\omega_n = u_{n+1} - u_n$ where $u_n = 2\tan^{-1}\{\tanh[-2n - \frac{t}{2\tanh(2)} + 0.3]\}$

If we let $u_n = 0$, n = 0 and 1, in Equation (2.22), then we have

$$0 = 2\tan^{-1}\left\{\tanh\left[-\frac{1}{2\tanh(k)}t + \zeta\right]\right\}, 0 = 2\tan^{-1}\{\tanh[k - \frac{1}{2\tanh(k)}t' + \zeta]\} \qquad (2.24)$$

the solution of these equations are

$$t = 2\tanh(k)(\zeta - i\pi N) \text{ and } t' = 2\tanh(k)(k + \zeta - i\pi N),\ \ N \in \mathbb{Z} \qquad (2.25)$$

Therefore, the velocity of the moving soliton in this system is

$$v = \frac{\Delta n}{\Delta t} = \frac{1-0}{t'-t} = \frac{1}{2k\tanh(k)} \qquad (2.26)$$

The sine-Gordon lattice structure of Equation (2.9) is shown in Fig. 2.12. There are one input u_n, one output u_{n+1}, one sine function and one integrator in this system making it simpler than the cell in Fig 2.2. The initial condition of the integrator is zero. The amplitude and frequency of the sine function are both one, while the bias and phase are

both zero. The way to connect these lattices is depicted in Fig. 2.13. From the analysis above we see that we conveniently can use the difference between u_n and u_{n+1} to transmit the signal in our sine-Gordon lattice system.

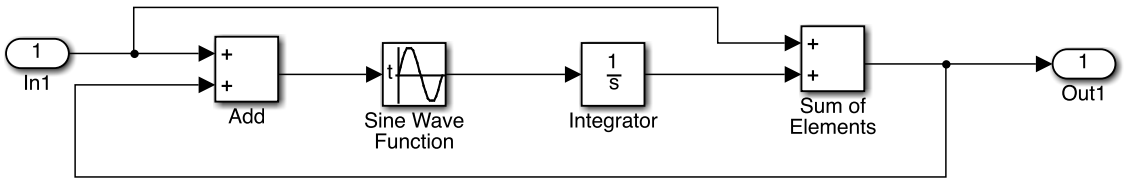

Fig. 2.12 Matlab Simulink model for Orfanidis's discrete sine-Gordon equation

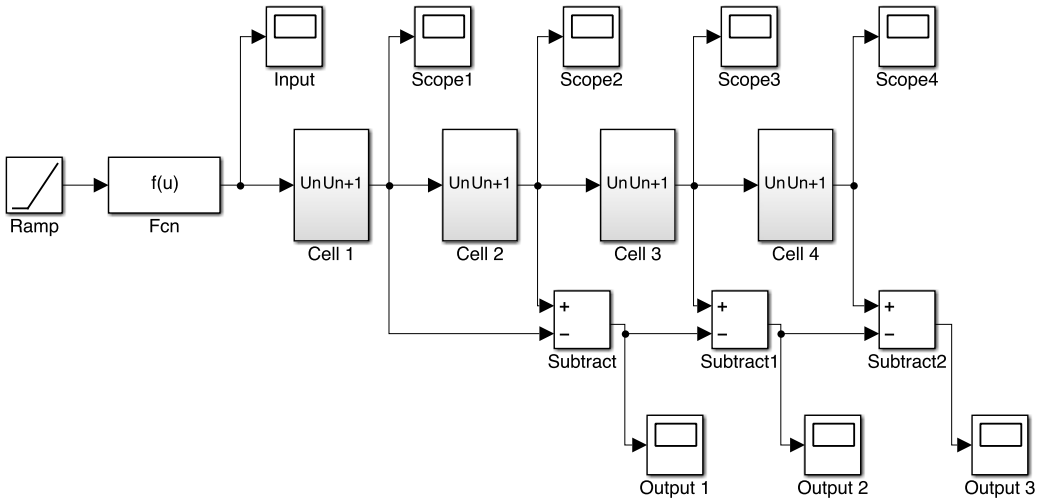

Fig. 2.13 The way to connect Orfanidis's discrete sine-Gordon equation models

The sine-Gordon lattice system with 45 cells is shown in Fig. 2.14 and its input $\mathrm{f}(u)|_{u=\mathrm{Ramp}}$ is

$$2\tan^{-1}\left\{\tanh\left[-\frac{t}{2\tanh(2)}+0.3\right]\right\},\ \ t>0 \tag{2.27}$$

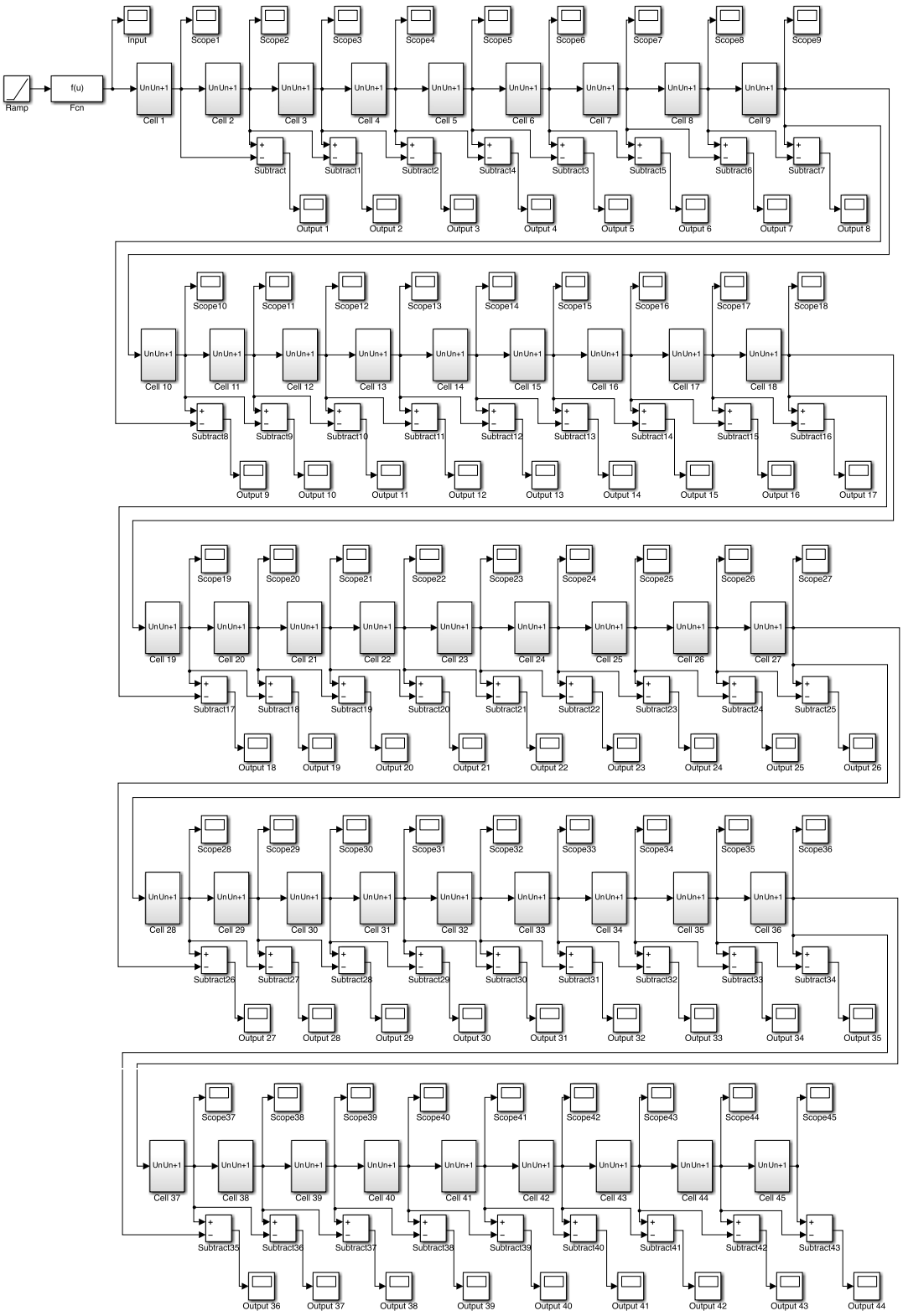

Fig. 2.14 The 45-lattice system for Orfanidis's discrete sine-Gordon equation

The plot of input signal is depicted in Fig. 2.15. The outputs of the cell 1, 9, 18, 27, 36, and 45 are shown in Fig. 2.16. From these output signals, we can see that to obtain the bell-type transmission signal, we should use the differences between the outputs of two successive cells.

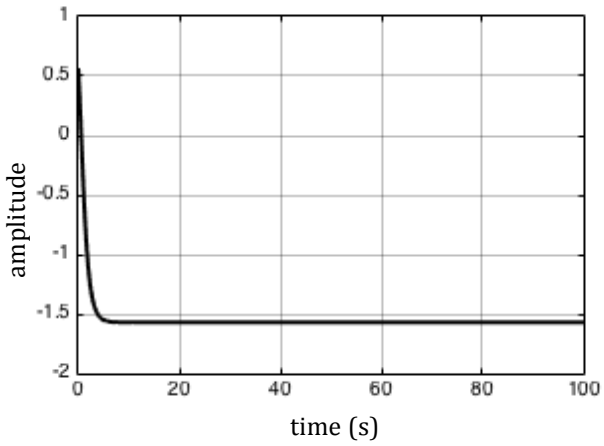

Fig. 2.15 The input of the 45-lattice system for Orfanidis's discrete sine-Gordon equation

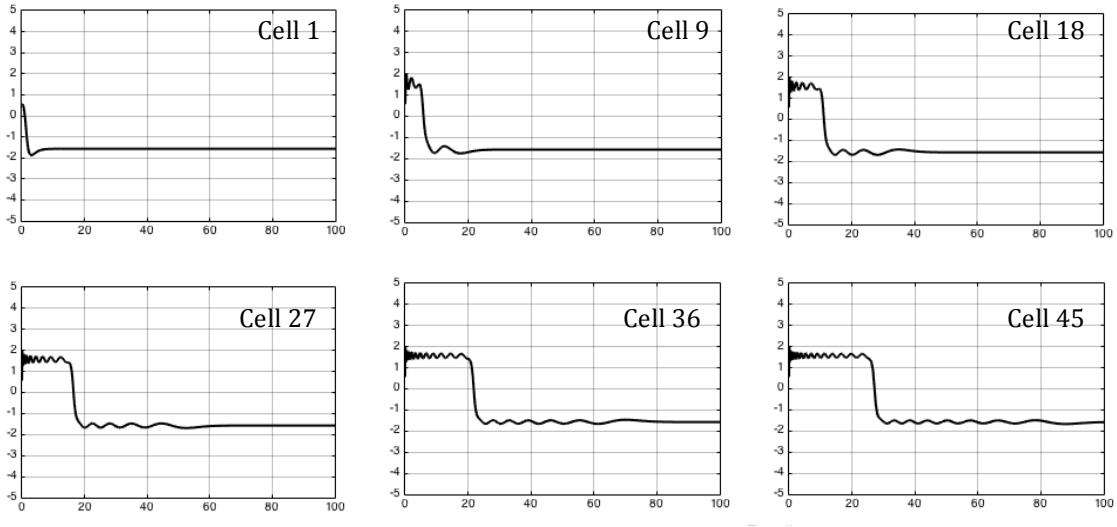

Fig. 2.16 The outputs of the cell 1, 9, 18, 27, 36, and 45 of the 45-lattice system where the x-axes are time and y-axes are amplitude

The outputs of the subtractor 1, 5, 9, 13, 17, 21, 24, 28, 32, 36, 40, and 44 are shown in Fig. 2.17 and they all contain the bell-type signals of almost the same shape and size and they are propagating constantly in the sine-Gordon lattice system. However, the shape of these signals are not well defined and not exactly bell-shaped.

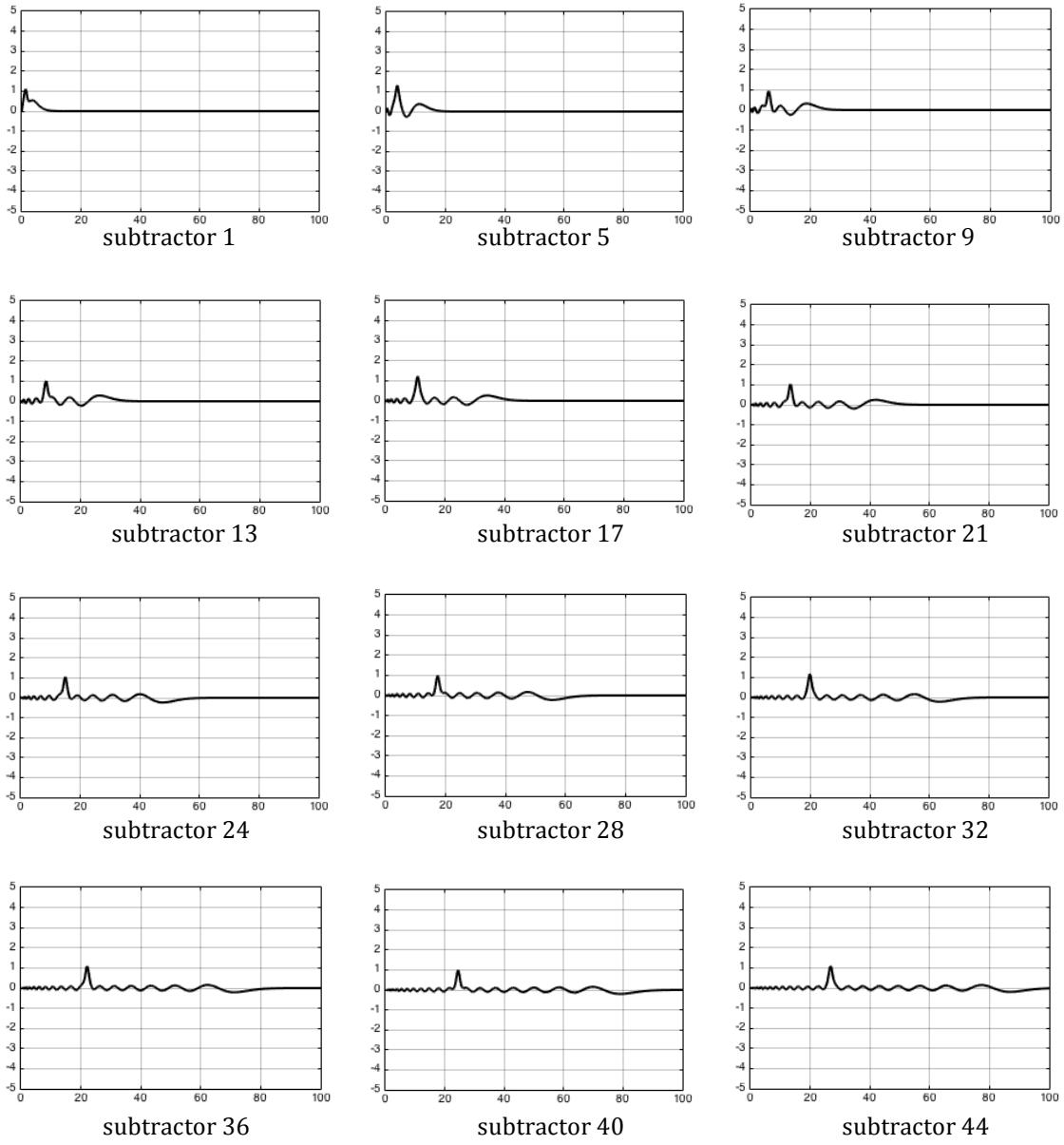

Fig. 2.17 The outputs of the subtractor 1, 5, 9, 13, 17, 21, 24, 28, 32, 36, 40, and 44 of the 45-lattice system where the x-axes are time and y-axes are amplitude

2.3 Sine-Lattice Equation

Takeno et al. showed that the sine-lattice equation with the difference factor $\sin(u_{n+1}-u_n)-\sin(u_n-u_{n-1})$ could sustain well-defined one-kink modes and no such similarity exists for the conventional discrete sine-Gordon equation with the difference factor $u_{n+1}+u_{n-1}-2u_n$ [10]. The sine-lattice equation is given by

$$\sin(u_{n+1}-u_n)-\sin(u_n-u_{n-1})-\frac{\mathrm{d}^2u_n}{\mathrm{d}t^2}=g\sin(u_n)\ ,\ n=0,\pm1,\pm2,\ldots \tag{2.28}$$

The 1-D nonlinear differential-difference equation is

$$\mathrm{f}(u_{n+1}-u_n)-\mathrm{f}(u_n-u_{n-1})-\frac{\mathrm{d}^2u_n}{\mathrm{d}t^2}=g\,\mathrm{v}(u_n) \tag{2.29}$$

and its 1-D lattice model has the Hamiltonian

$$H=\sum_n\frac{\dot{u}_n^2}{2}+\sum_n\mathrm{F}(u_{n+1}-u_n)+g\sum_n V(u_n) \tag{2.30}$$

where

$$F(u)=-\int_{-\infty}^{u}f(u')\mathrm{d}u'+\mathrm{const}\,,\ \text{and}\ V(u)=-\int_{-\infty}^{u}v(u')\mathrm{d}u'+\mathrm{const} \tag{2.31}$$

are inter-site and on-site potentials respectively. Equation (2.28) is a specific form of Equation (2.29) for a lattice model with the Hamiltonian

$$H=\sum_n\frac{\dot{u}_n^2}{2}+\sum_n[1-\cos(u_{n+1}-u_n)]+g\sum_n(1-\cos u_n) \tag{2.32}$$

By introducing the Hirota bilinear operator, Takeno et al. found the exact soliton solution to Equation (2.28) and it is given by

$$u=4\tan^{-1}(a/b) \tag{2.33}$$

and for the one-kink solution

$$a=e^{\eta},\ \text{and}\ b=1 \tag{2.34}$$

where

$$\eta = kx + \omega t + \eta_0 \equiv kn + \omega t + \eta_0 \tag{2.35}$$

where k and ω are kink momentum and frequency, respectively, and η_0 is a constant. Therefore the kink velocity v is ω/k. From Equation (2.33), (2.34), and (2.35), the solution of the sine-lattice equation becomes

$$u = 4\tan^{-1}(e^{kn+\omega t+\eta_0}) \tag{2.36}$$

The Matlab plots of space-time evolution of

$$\omega_n(t) \equiv u_{n+1}(t) - u_n(t) \tag{2.37}$$

are shown in Fig. 2.18 and Fig. 2.19 with k ≃1 and ω=-0.1.

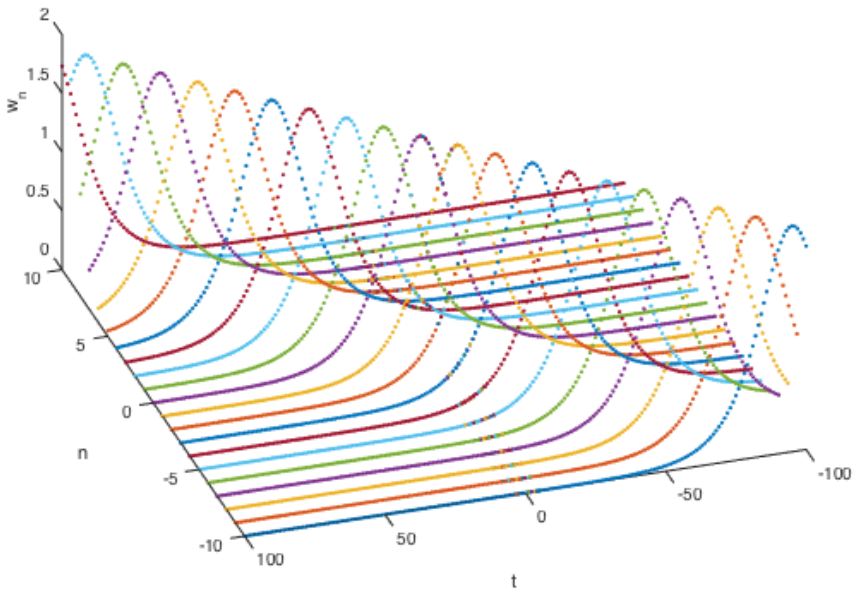

Fig. 2.18 Matlab space-time evolution plot of $\omega_n = u_{n+1} - u_n$ when -10<n<10

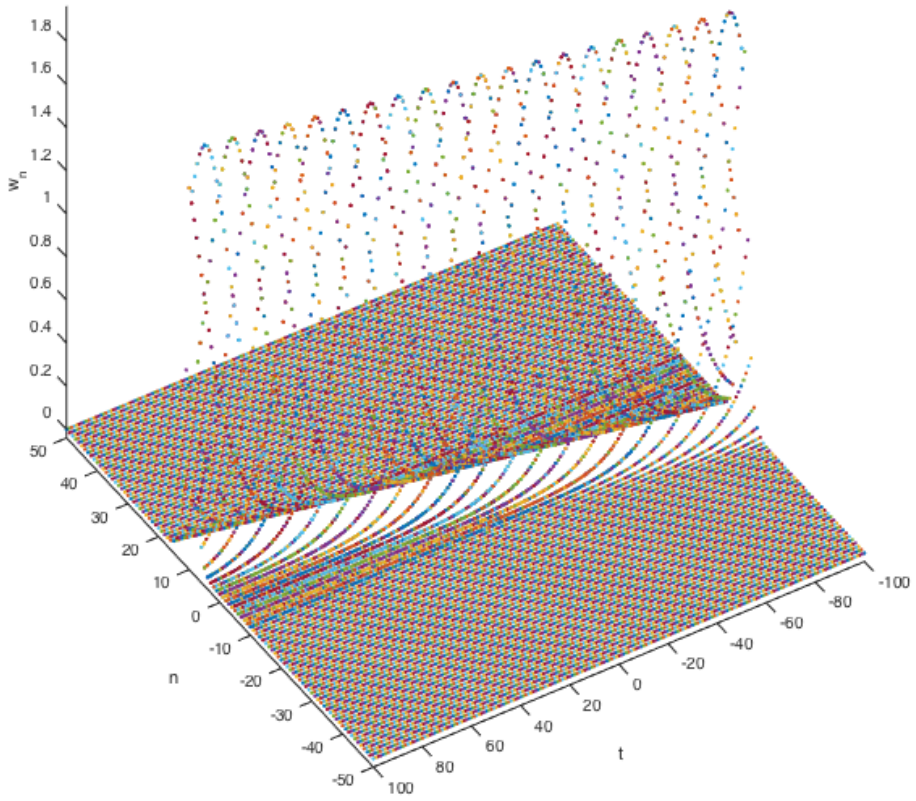

Fig. 2.19 Matlab space-time evolution plot of $\omega_n = u_{n+1} - u_n$ when -50<n<50

The sine-Gordon lattice structure of Equation (2.28) is shown in Fig. 2.20. There are two inputs u_{n+1} and u_{n-1}, one output u_n, three sine functions and two integrators in this system. The initial conditions of two integrators are both zero. The frequencies of the three sine functions are 1, while the biases and phases are zero. The amplitudes of sine function2 is 0.1 since when we let g = 0.1 in Equaiton (2.28) the system gives best results. The other two sine functions have the amplitudes of one. The way to connect these lattices is shown in Fig. 2.21. The input u_{n+1} of the last cell is zero. From the space-time evolution plots of $\omega_n(t)$ shown in Fig. 2.18 and Fig. 2.19, we can conclude that $\omega_n(t)$ should be used as the transmission signal in sine-Gordon lattice system.

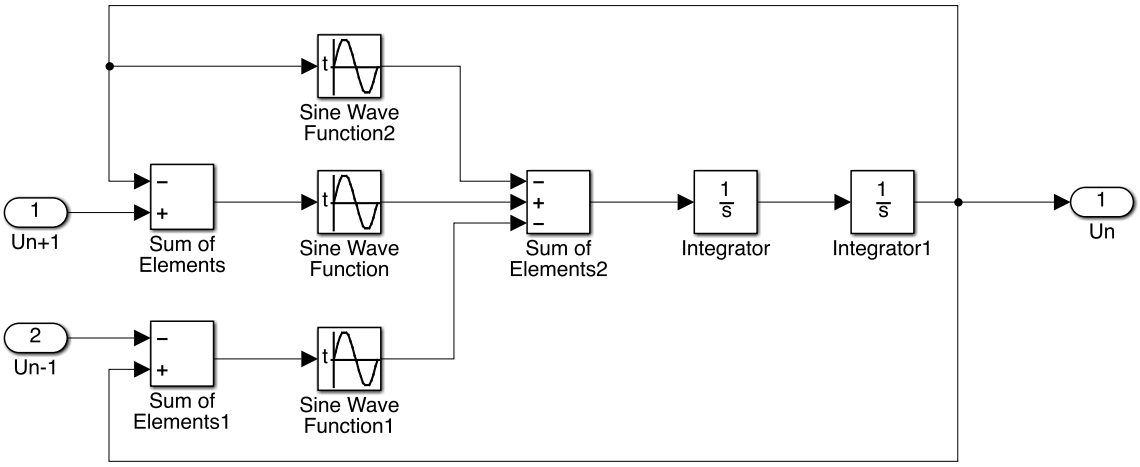

Fig. 2.20 Matlab Simulink model for sine-lattice equation

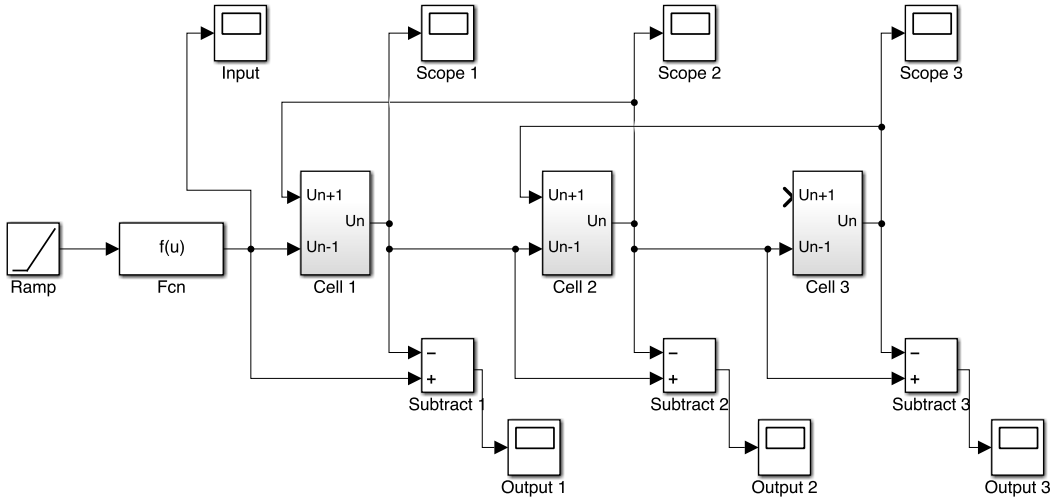

Fig. 2.21 The way to connect sine-lattice equation models

The sine-Gordon lattice system with 72 cells is shown in Fig. 2.22. The input of this system is

$$4\tan^{-1}(e^{32-0.5t}) \tag{2.38}$$

since it gives the best results and the plot of this input signal is depicted in Fig. 2.23.

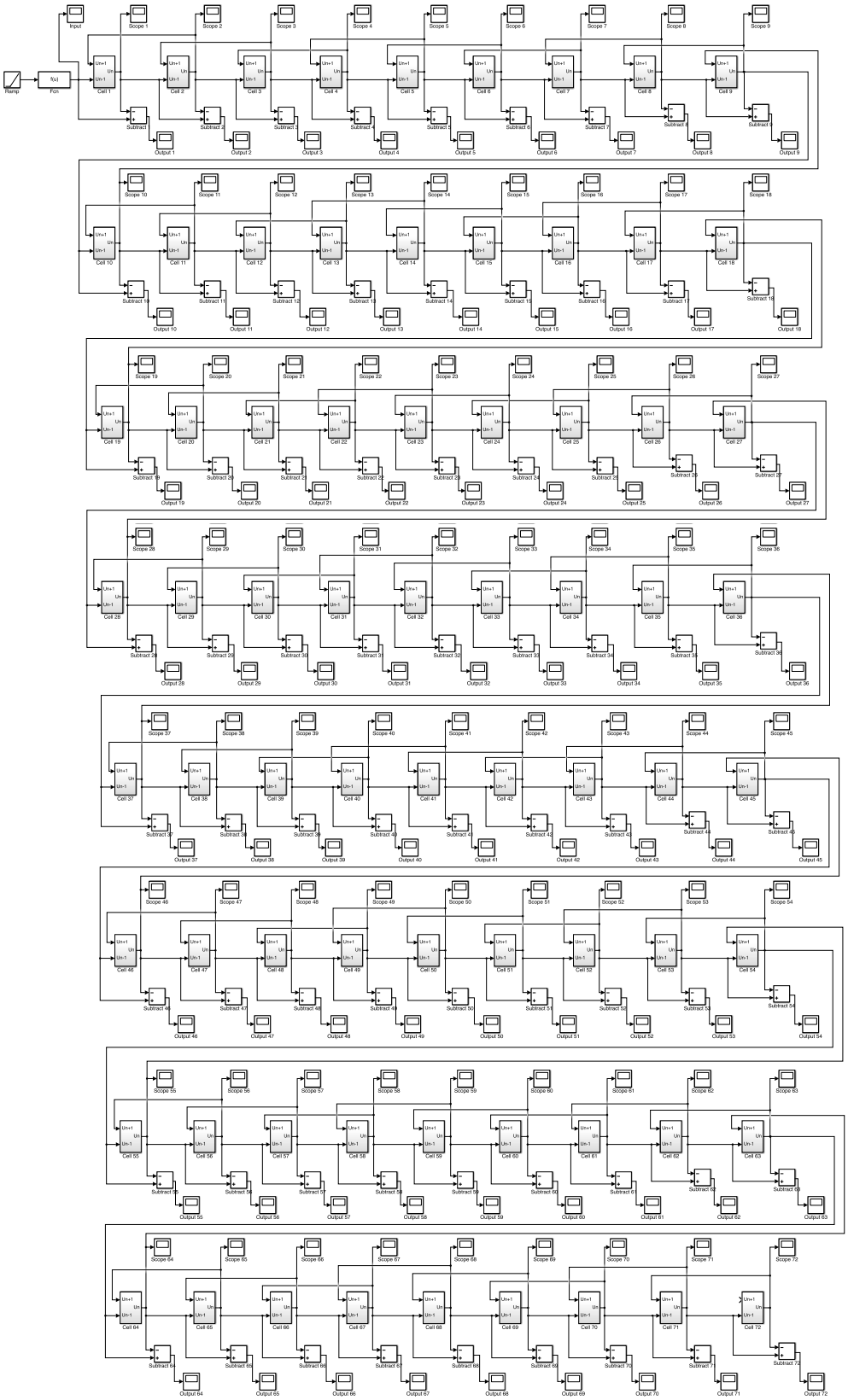

Fig. 2.22 The 72-lattice system for sine-lattice equation

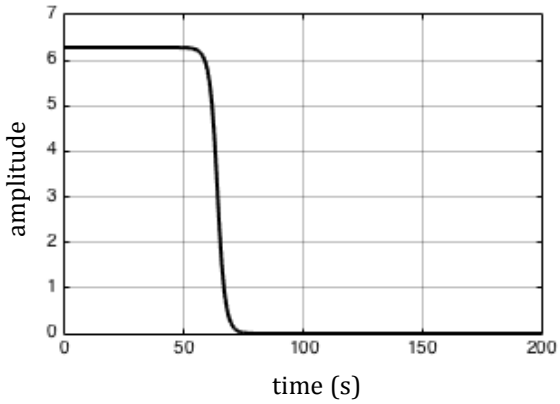

Fig. 2.23 The input of the 72-lattice system for sine-lattice equation

The outputs of the cell 1, 19, 37, 55, 60, 64, 68, and 72 are shown in Fig. 2.24. From these output signals and the analysis above, we see that to obtain the bell-type transmission signal, again we should use the difference ω_n between the outputs u_{n+1} and u_n of successive cells. The outputs of the subtractor 2, 5, 9, 14, 18, 23, 27, 32, 36, 41, 45, 50, 54, 59, 63, and 72 are shown in Fig. 2.25 and they are all bell-type signals of the same shape and size and propagate with constant velocity along the transmission path of the sine-Gordon lattice system.

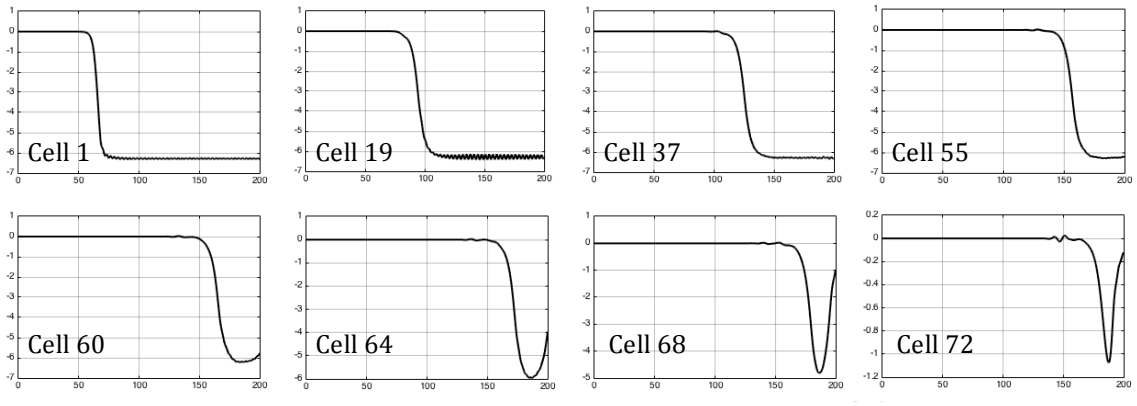

Fig. 2.24 The outputs of the cell 1, 19, 37, 55, 60, 64, 68, and 72 of the 72-lattice system where the x-axes are time and y-axes are amplitude

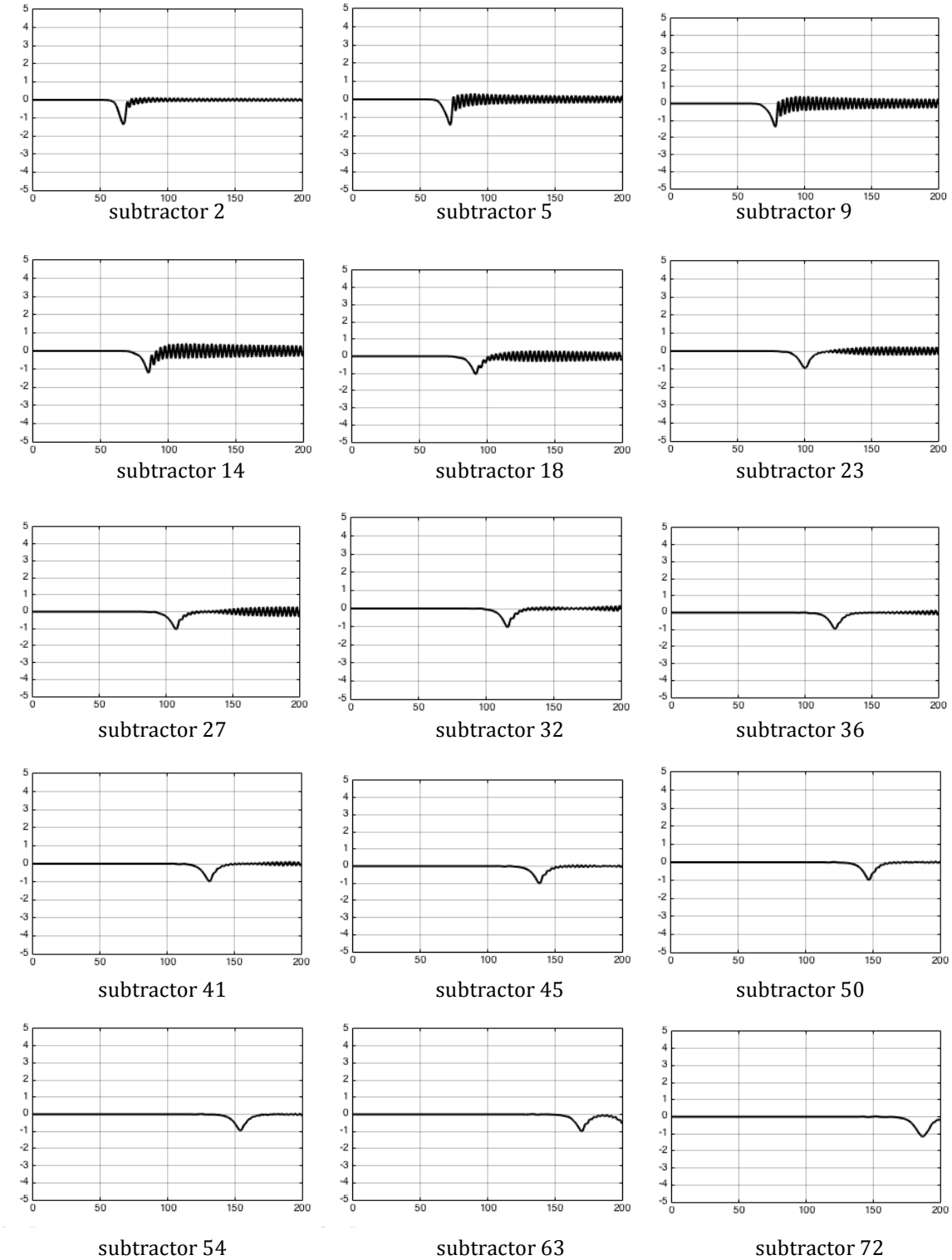

Fig. 2.25 The outputs of the subtractor 2, 5, 9, 14, 18, 23, 27, 32, 36, 41, 45, 50, 54, 63, and 72 of the 72-lattice system where the x-axes are time and y-axes are amplitude

The simulation results show that the sine-lattice equation system has better performance in transmitting soliton signals than the conventional discrete sine-Gordon equation system and Orfanidis's discrete sine-Gordon equation system. Even though with well-defined soliton transmission, the basic cell of the sine-lattice equation system contains three sine functions; this is a major downside in terms of application. However, if we change the structure of the basic cell, namely with two inputs $\sin(u_n-u_{n-1})$, u_{n+1}, and two outputs $\sin(u_{n+1}-u_n)$, u_n, than we could reduce the number of sine functions form three to two. The equations for this 2-sine cell are

$$o_1 = \sin(i_1 - o_2) \tag{2.39}$$

$$o_2 = \iint_{-\infty}^{\infty} [i_1 - o_1 - g\sin(o_2)] \tag{2.40}$$

where i_1 is $\sin(u_n-u_{n-1})$, i_2 is u_{n+1}, o_1 is $\sin(u_{n+1}-u_n)$, and o_2 is u_n. The new cell structure is shown in Fig. 2.26. In Fig. 2.27, when connecting these cells, we need an extra sine function at the input of the first cell. The input u_{n+1} of the last cell is zero. Since the sine-Gordon lattice systems in Fig. 2.20 and Fig. 2.26 realize the same sine-lattice equation (2.28), the simulation results should also be the same.

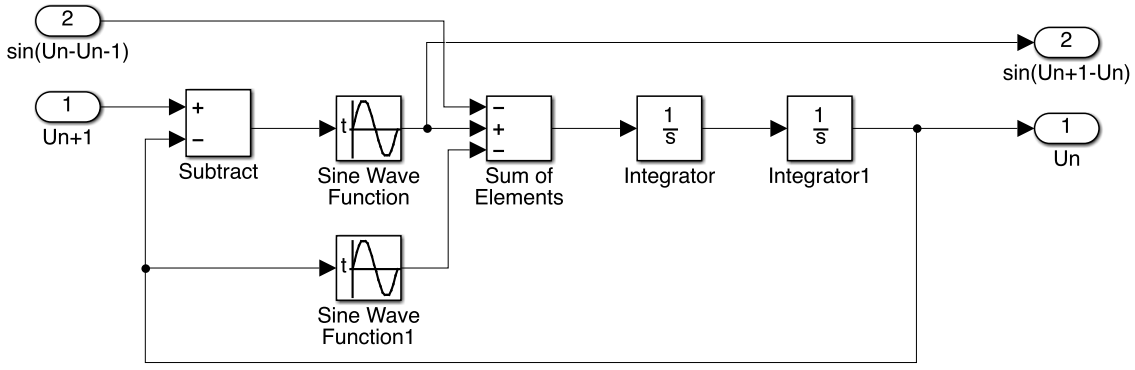

Fig. 2.26 Matlab Simulink model for sine-lattice equation with two sine functions

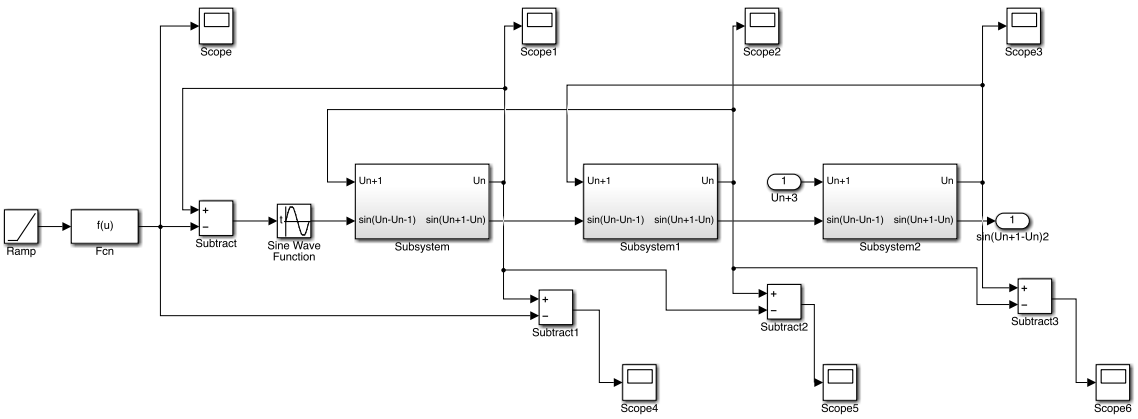

Fig. 2.27 The way to connect the two-sine sine-lattice equation models

2.4 Conclusions

From the Matlab Simulink simulation results of the three discrete sine-Gordon equation lattice systems, we see that if we take the difference between the outputs of two successive cells as the transmitting signal, all three systems can propagate this signal constantly without too much amplitude loss and distortion. For the conventional discrete sine-Gordon system, although the signal is bell-type, there are many other relatively large signals as well. For Orfanidis's discrete sine-Gordon equation system, while the noise is small, the transmission signal is not exactly bell-shaped. The sine-lattice equation system gives the best results among the three systems. The bell-shaped propagating signal preserves the size and shape along the transmission while the noise signals are low compered to the transmission signal. And therefore, we prefer to use the sine-lattice equation to construct the sine-Gordon lattice system.

Chapter 3 sin(x)-Circuit

In the Sine-Gordon Lattice designs, we have at least one sine function that takes the signal u_n as input and generates $\sin(u_n)$ as output. There are many ways to construct the sin(x)-circuit and many of them are translinear circuits consisting of bipolar transistors or MOS transistors under weak inversion. In this chapter, we will first discuss some translinear circuits and simulate the MOS translinear sin(x)-circuits discussed in Mulder's paper[16]. Then, we will create the complete circuit for the cell of the third sine-Gordon lattice system in chapter 2 using the sin(x)-circuits mentioned above.

3.1 Background of sin(x)-Circuit

In this part, we will discuss the translinear principle and some basic bipolar and MOS translinear circuits. We will also introduce several translinear circuits that realize sin(x) function.

3.1.1 Tanslinear Circuits

The first translinear circuits were proposed in Gilbert's paper in 1974 [11]. Translinear circuits used here only take currents as inputs and outputs and, therefore, work entirely in the current domain. The bipolar transistor translinear circuits make use of the linear relationship between transconductance and collector current. If the base-emitter junction of an npn bipolar transistor is driven by the applied voltage V_{BE}, then the collector current is

$$I_C = A_E J_S(T) e^{V_{BE}/nV_T} \tag{3.1}$$

where A_E is the emitter area and $J_S(T)$ is the saturation current density. The derivative of the collector current function (3.1) with respect to V_{BE} is

$$\frac{\partial I_C}{\partial V_{BE}} = g_m = \frac{I_C}{V_T} \tag{3.2}$$

And we can see that the transconductance of the ideal bipolar transistor is a linear function of the collector current. Nowadays, the translinear circuits consist of devices with exponential behavior, including all bipolar transistors and MOS transistors operated in the subthreshold region [12]. The translinear principle is stated below:

"In a closed loop containing an even number of ideal junctions, arranged so that there are an equal number of clockwise-facing and counter-clockwise-facing polarities, with no further voltage generators inside this loop, the product of the current densities in the clockwise direction is equal to the product of the current densities in the counter-clockwise direction. [12]"

The translinear principle can be written in this form

$$\prod_{CW} J = \prod_{CCW} J \tag{3.3}$$

The classic translinear circuit is the quadruple of transistors shown in Fig. 3.1.

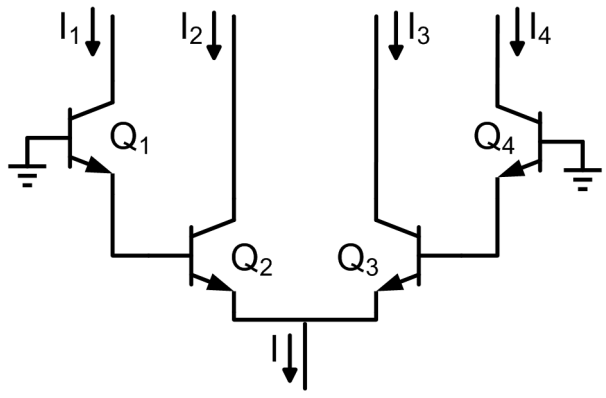

Fig. 3.1 Basic translinear quadrupe of bipolar transistors

From the translinear principle above and neglecting base currents, we have

$$J_1 J_2 = J_3 J_4 \tag{3.4}$$

If the emitter areas of are all equal, then we have

$$I_1 I_2 = I_3 I_4 \tag{3.5}$$

Depending on different driving methods, this circuit can be used as a multiplier, divider, squarer, square-rooter, r.m.s. convertor, and so on [11]. For example, a four-transistor 4-quadrant multiplier is showed in Fig. 3.2, the input currents are given by

$$I_{in1} = \frac{(1+X)I}{2}, I_{in2} = \frac{(1-X)I}{2}, \text{and } I_r = (1+Y)I \tag{3.6}$$

where I is the refernce current and X, Y are the inputs of this 4-quadrant multiplier.

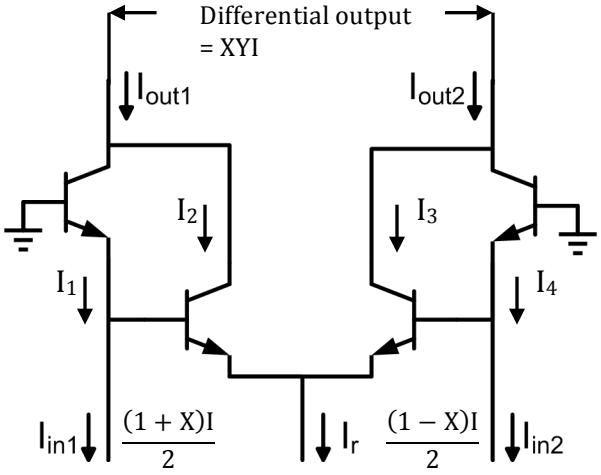

Fig. 3.2 Four-BJT 4-quadrant tanslinear multiplier

From Fig. 3.2, we have

$$I_2 + I_3 = (1+Y)I \tag{3.7}$$

Since $I_1 = I_{in1}$ and $I_4 = I_{in2}$, solving two Equations (3.5), (3.6), and (3.7) above, we get the solutions for I_2 and I_3

$$I_2 = \frac{(1-X)(1+Y)I}{2}, \text{and } I_3 = \frac{(1+X)(1+Y)I}{2} \tag{3.8}$$

Since the input current and output current are

$$I_{in} = I_{in1} - I_{in1} = XI, \text{and } I_{out} = I_{out2} - I_{out1} = (I_1 + I_2) - (I_3 + I_4) \tag{3.9}$$

Therefore, the differrential output current is

$$I_{out} = \frac{(1+X)I}{2} + \frac{(1-X)(1+Y)I}{2} - \frac{(1+X)(1+Y)I}{2} - \frac{(1-X)I}{2} = XYI \tag{3.10}$$

3.1.2 MOS Translinear Circuits

Besides bipolar transistors, due to the exponential characteristics, MOS transistors also can be applied to the translinear circuits design when operating in weak inversion. There are two major differences between the BJT translinear circuits and MOS translinear circuits. First, the current in the MOS transistor, unlike the bipolar transistor, is controlled by the surface potential difference between the channel surface potential and the potential at the source or drain. Second, the MOS transistor normally has symmetric drain and source terminals while a bipolar transistor does not [13]. The current between the drain and source of an NMOS is given by [14]

$$I_{DS} = I_0 \frac{W}{L} e^{\kappa V_{GS}/V_T} e^{(1-\kappa)V_{BS}/V_T} \left(1 - e^{-V_{DS}/V_T}\right) \tag{3.11}$$

When the MOS transistor is in saturation, i.e.

$$V_{DS} > 4V_T \tag{3.12}$$

then the equation for the drain current of MOS transistor is given by

$$I_{DS} = I_0 \frac{W}{L} e^{\frac{(1-\kappa)V_{BS}}{V_T}} e^{\frac{\kappa V_{GS}}{V_T}} \tag{3.13}$$

If we short the bulk and the source of the transistor, i.e. V_B=V_S, then we have

$$I_{DS} = I_0 \frac{W}{L} e^{\frac{\kappa V_{GS}}{V_T}} \tag{3.14}$$

A simple example of a PMOS translinear circuit is shown in Fig. 3.3, which performs one-quadrant normalized multiplication and exploits the back-gate in a MOS transistor [13]. From Equation (3.13), the four drain currents are

$$I_1 = I_0 \frac{W}{L} e^{\frac{(1-\kappa_1)V_{SB1}}{V_T}} e^{\frac{\kappa_1 V_{SG1}}{V_T}} \tag{3.15a}$$

$$I_2 = I_0 \frac{W}{L} e^{\frac{(1-\kappa_1)V_{SB2}}{V_T}} e^{\frac{\kappa_1 V_{SG2}}{V_T}} \tag{3.15b}$$

$$I_3 = I_0 \frac{W}{L} e^{\frac{(1-\kappa_1)V_{SB3}}{V_T}} e^{\frac{\kappa_1 V_{SG3}}{V_T}} \tag{3.15c}$$

$$I_4 = I_0 \frac{W}{L} e^{\frac{(1-\kappa_1)V_{SB4}}{V_T}} e^{\frac{\kappa_1 V_{SG4}}{V_T}} \tag{3.15d}$$

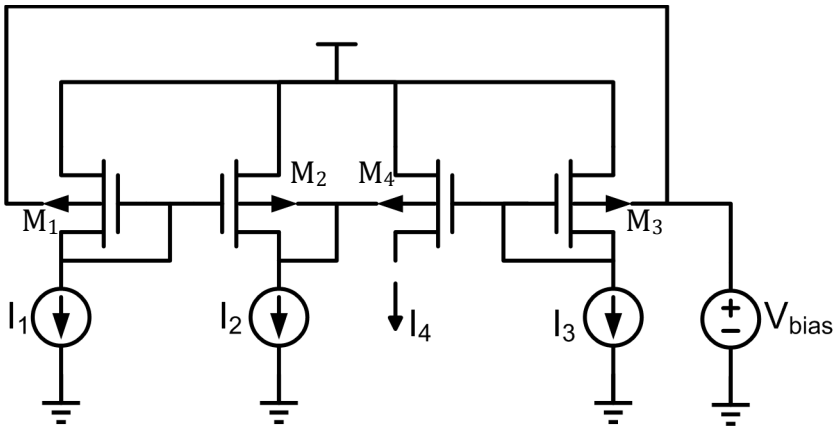

Fig. 3.3 Four-MOS transistor translinear one-quadrant multiplier

The voltages on the gate and bulk control the drain currents according to the Equation (3.13). And since the device pairs M1, M3 and M2, M4 share the same back-gates and device pairs M1, M2 and M3, M4 share the same front gates, then we have

$$V_{SG1} = V_{SG2}, V_{SG3} = V_{SG4}, V_{SB2} = V_{SB4}, V_{SB1} = V_{SB3} \tag{3.16}$$

If we assume that $\kappa_1 = \kappa_2 = \kappa_3 = \kappa_4$, then we have

$$\mathrm{I_1 I_2} = \mathrm{I_3 I_4} \tag{3.17}$$

And therefore the output current is

$$\mathrm{I_4} = \frac{\mathrm{I_1 I_2}}{\mathrm{I_3}} \tag{3.18}$$

3.1.3 MOS Translinear Circuits Using Back Gates

An MOS transistor is a four-terminal device. However, its bulk is often connected to the source and therefore the MOS transistor is usually used as a three-terminal device. To demonstrate the usefulness of the back-gate of MOS transistor operating in subthreshold region, Mulder et al. [5] experimented on the bulk current-mirror. In the conventional current-mirror [15] shown in Fig. 3.4, the bulk and source are shorted, and the input current forces the gate voltage. However, for the bulk current-mirror shown in Fig. 3.5, the gate voltage is constant and the bulk is used to mirror the input current. Since the slope of V_{BS} – ln(I_{DS}) is about twice as steep as the slope of V_{GS}-ln(I_{DS}), an improved bulk current mirror shown in Fig. 3.6 was introduced, where M_3 serves as a voltage source and the bias current I_b is much smaller than I_{in} [5].

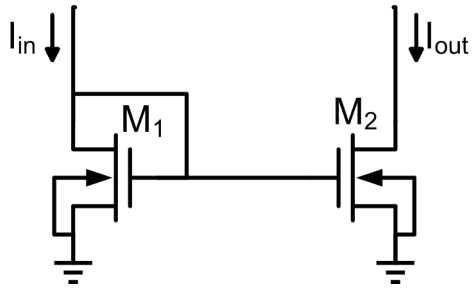

Fig. 3.4 Conventional current mirror

In Fig. 3.5, since the sources of M_1 and M_2 are grounded and the drains of the two transistors are driven by a common voltage source V_b, from Equation (3.13), the drain currents are given by

$$I_{in} = I_0 \frac{W}{L} e^{\frac{(1-\kappa)V_{B1}}{V_T}} e^{\frac{\kappa V_b}{V_T}} \tag{3.19a}$$

$$I_{out} = I_0 \frac{W}{L} e^{\frac{(1-\kappa)V_{B2}}{V_T}} e^{\frac{\kappa V_b}{V_T}} \tag{3.19b}$$

Similarly, the reference current in Fig. 3.6 is given by

$$I_b = I_0 \frac{W}{L} e^{\frac{\kappa(V_b - V_{B3})}{V_T}} \tag{3.19c}$$

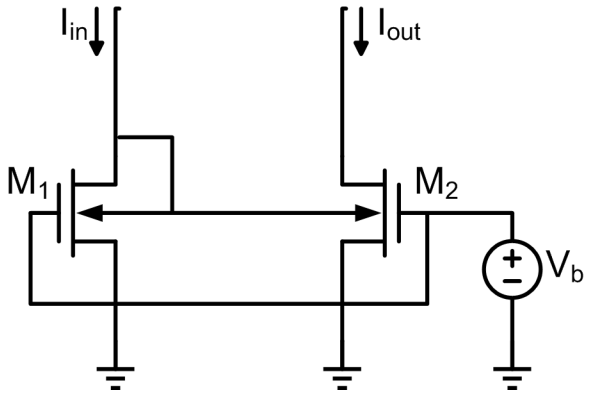

Fig. 3.5 Bulk current mirror

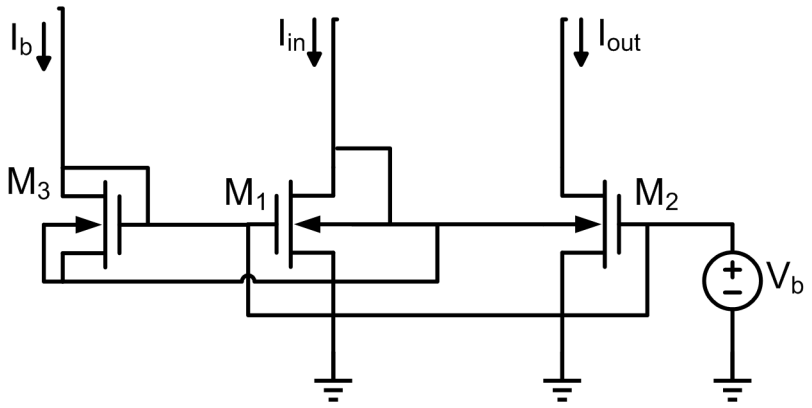

Fig. 3.6 Improved bulk current mirror

In Fig. 3.5, the bulks of M_1 and M_2 are connected together, so we have $V_{B1} = V_{B2}$, and therefore we have

$$I_{in} = I_{out} \tag{3.20}$$

Similarly, in Fig. 3.6, the bulks of M_1, M_2, and M_3 are connected together, so we have $V_{B1} = V_{B2} = V_{B3} = V_B$, and therefore we have

$$I_{in} = I_{out} = I_b e^{\frac{\kappa V_B}{V_T}} \tag{3.21}$$

Mulder's experimental results about the bulk current mirror and improved bulk current mirror showed that by exploiting the back gate of an MOS transistor under weak inversion, the MOS translinear circuits can work at very low voltage and low current, and can be used for low-voltage and low-power applications [16].

3.1.4 Translinear Sine Circuits

In the first paper about translinear circuits, Gilbert described a bipolar translinear circuits that generates the sin(πx) function [11]. In Greeneich's book [17], he introduced a similar translinear sine circuit shown in Fig. 3.7. The input currents of this sine circuit are

$$\mathrm{I}_{in1} = \frac{(1+X)\mathrm{I}}{2}, \text{and } \mathrm{I}_{in2} = \frac{(1-X)\mathrm{I}}{2} \tag{3.22}$$

where I is the refernce current and X, Y are the inpus of this 4-quadrant multiplier. And therefore the differential input current is

$$\mathrm{I}_{in}=\mathrm{I}_{in1}-\mathrm{I}_{in2}=X\mathrm{I} \tag{3.23}$$

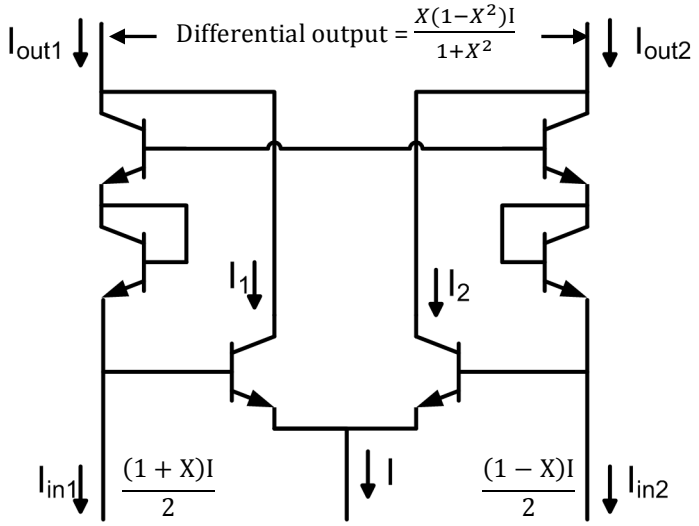

Fig. 3.7 Sine approximation translinear circuit

If the emitter areas of are all equal, from the translinear principle we have

$$\mathrm{I}_{in1}^2\mathrm{I}_1=\mathrm{I}_2\mathrm{I}_{in2}^2 \tag{3.24}$$

From Equation (3.22) and Equation (3.24), we have

$$\left(\frac{(1+X)\mathrm{I}}{2}\right)^2 I_1=I_2\left(\frac{(1-X)\mathrm{I}}{2}\right)^2 \tag{3.25}$$

From Fig. 3.7, we find the relation

$$I_1+I_2=I \tag{3.26}$$

Solving two Equations (3.25) and (3.26) above, we get the solutions for I_2 and I_3

$$I_1=\frac{(1-X)^2I}{2(1+X^2)}, \text{and } I_2=\frac{(1+X)^2I}{2(1+X^2)} \tag{3.27}$$

Since the output current is given by

$$I_{out1} = I_{in1} + I_1, I_{out2} = I_{in2} + I_2, \text{ and } I_{out} = I_{out2} - I_{out1} \tag{3.28}$$

Therefore, using the expressions for I_1 and I_2 in Equation (3.27), the differrential output current is of the form

$$I_{out} = \frac{(1-X)I}{2} + \frac{(1+X)^2 I}{2(1+X^2)} - \frac{(1+X)I}{2} - \frac{(1-X)^2 I}{2(1+X^2)} = \frac{X(1-X^2)\mathrm{I}}{1+X^2} \tag{3.29}$$

When -1 < X < 1, then we have [11]

$$\frac{X(1-X^2)}{1+X^2} \simeq \sin(\pi X) \tag{3.30}$$

This bipolar translinear circuit could output a good approximation (the maximum error is about 3%) to the sin function current over the range [-π, π] [17].

Gilbert also introduced two sine circuits in 1977 [18] and 1982 [19] by realizing the sum of series of equally spaced hyperbolic tangent functions and the sum of series of parabolic spaced exponential functions respectively in the bipolar translinear circuits. Fried and Enz described a MOS translinear circuit that generates sine-shaped differential output current [20]. This sin(x) shaper is depicted in Fig. 3.8 and it takes the voltage difference as the input instead of the current in the conventional translinear circuits.

When the MOS trasistors are in saturation and working in the subthreshold region, the equations for the two output currents are

$$I_1 = I_o \frac{W}{L} e^{\frac{(1-\kappa_1)V_{BS1}}{V_T}} e^{\frac{\kappa_1 V_{GS1}}{V_T}} \tag{3.31a}$$

$$I_2 = I_o \frac{W}{L} e^{\frac{(1-\kappa_2)V_{BS2}}{V_T}} e^{\frac{\kappa_2 V_{GS2}}{V_T}} \tag{3.31b}$$

The output current and the tail currents are

$$I_o = I_1 - I_2, \text{and } I_q = I_1 + I_2 \tag{3.32}$$

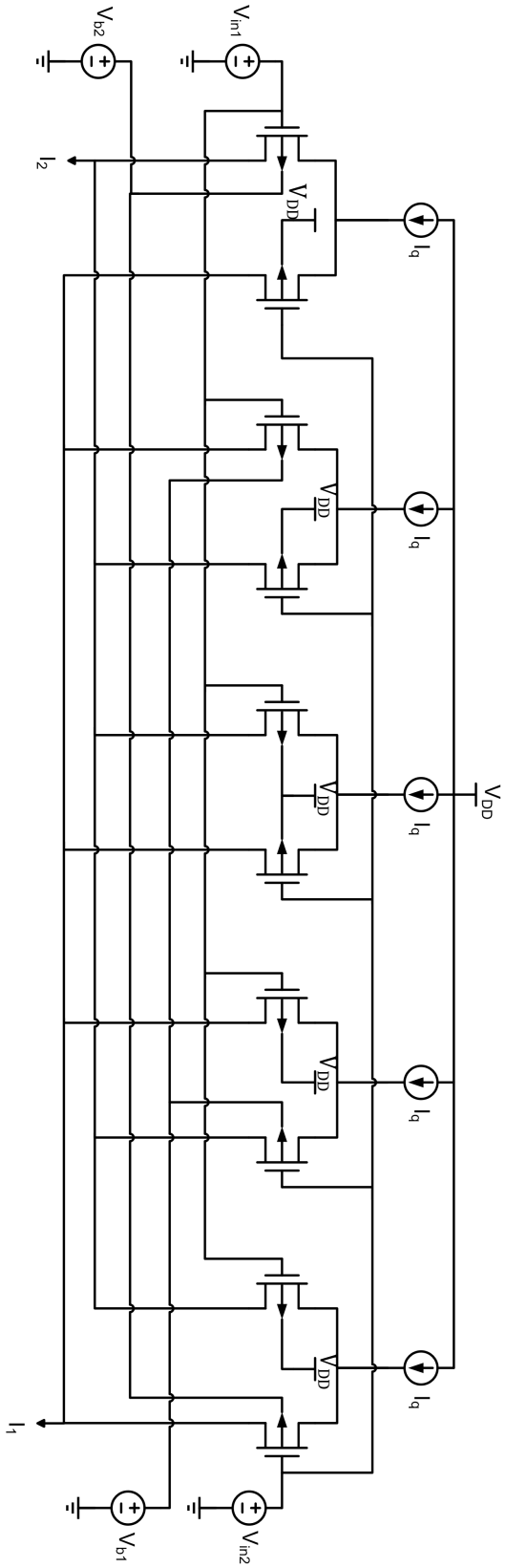

Fig. 3.8 MOS translinear sin(x) shaper

Then taking the ratio of these two currents

$$\frac{I_o}{I_q}=\frac{I_1-I_2}{I_1+I_2}=\frac{e^{\frac{(1-\kappa_1)V_{BS1}}{V_T}}e^{\frac{\kappa_1 V_{GS1}}{V_T}}-e^{\frac{(1-\kappa_2)V_{BS2}}{V_T}}e^{\frac{\kappa_2 V_{GS2}}{V_T}}}{e^{\frac{(1-\kappa_1)V_{BS1}}{V_T}}e^{\frac{\kappa_1 V_{GS1}}{V_T}}+e^{\frac{(1-\kappa_2)V_{BS2}}{V_T}}e^{\frac{\kappa_2 V_{GS2}}{V_T}}} \tag{3.33}$$

Let $\kappa_1=\kappa_2=\kappa$ and $V_{S1}=V_{S2}$ by connecting their sources together, then Equation (3.33) becomes

$$\frac{I_o}{I_q}=\frac{e^{\frac{(1-\kappa)V_{B1}}{V_T}}e^{\frac{\kappa V_{G1}}{V_T}}-e^{\frac{(1-\kappa)V_{B2}}{V_T}}e^{\frac{\kappa V_{G2}}{V_T}}}{e^{\frac{(1-\kappa)V_{B1}}{V_T}}e^{\frac{\kappa V_{G1}}{V_T}}+e^{\frac{(1-\kappa)V_{B2}}{V_T}}e^{\frac{\kappa V_{G2}}{V_T}}} \tag{3.34}$$

If we divide the denominator and numerator of the right-hand side of the Equation (3.34) by

$$e^{\frac{(1-\kappa)V_{B1}+\kappa V_{G1}}{2V_T}+\frac{(1-\kappa)V_{B2}+\kappa V_{G2}}{2V_T}} \tag{3.35}$$

Then we have

$$\frac{I_o}{I_q}=\frac{e^{\frac{(1-\kappa)V_{B1}+\kappa V_{G1}}{2V_T}-\frac{(1-\kappa)V_{B2}+\kappa V_{G2}}{2V_T}}-e^{-\frac{(1-\kappa)V_{B1}+\kappa V_{G1}}{2V_T}+\frac{(1-\kappa)V_{B2}+\kappa V_{G2}}{2V_T}}}{e^{\frac{(1-\kappa)V_{B1}+\kappa V_{G1}}{2V_T}-\frac{(1-\kappa)V_{B2}+\kappa V_{G2}}{2V_T}}+e^{-\frac{(1-\kappa)V_{B1}+\kappa V_{G1}}{2V_T}+\frac{(1-\kappa)V_{B2}+\kappa V_{G2}}{2V_T}}} \tag{3.36}$$

$$\frac{I_o}{I_q}=\tanh\left(\frac{(1-\kappa)V_{B1}+\kappa V_{G1}-(1-\kappa)V_{B2}-\kappa V_{G2}}{2V_T}\right) \tag{3.37}$$

The sine function can be implemented by the sum of hyperbolic tangents for the angular range of [-mπ, mπ] and it is given by [18]

$$\sum_{k=-m}^{m}(-1)^k\tanh(x+k\alpha)\rightarrow\beta\sin(\frac{\pi x}{\alpha}) \tag{3.38}$$

where β is an amplitude factor and is given by

$$\beta=\frac{4\pi}{\alpha}e^{\frac{-\pi^2}{2\alpha}} \tag{3.39}$$

From Equation (3.37) and Equation (3.38), we find that

$$\alpha = \frac{(1-\kappa)(V_{B1}-V_{B2})}{2V_T}, \text{ and } x = \frac{\kappa(V_{G1}-V_{G2})}{2V_T} \tag{3.40}$$

for each differential pairs. The positive and negative offsets in the differential pairs can be introduced by the aspect ratios or bulk voltages and both simulation results [20] showed that the differential output current I_{out} is a sine function of the differential input voltage V_{in}.

3.2 Principle of Operation of MOS Translinear sin(x)-Circuits

The drain current equation of an NMOS transistor operating in the subthreshold region is given by Equation (3.11), i.e.

$$I_{DS} = I_0 \frac{W}{L} e^{\kappa V_{GS}/V_T} e^{(1-\kappa)V_{BS}/V_T}\left(1 - e^{-V_{DS}/V_T}\right) \tag{3.11}$$

where $V_T = KT/q$ is the thermal voltage, W is the transistor width, L is its length, I_0 is a positive constant current, and κ is a technology-dependent positive parameter. If the MOS transistor is working in the saturation region i.e. when Equation (3.12) satisfies, i.e.

$$V_{DS} > 4V_T \tag{3.12}$$

then, Equation (3.11) can be simplified to Equation (3.13), i.e.

$$I_{DS} = I_0 \frac{W}{L} e^{\kappa V_{GS}/V_T} e^{(1-\kappa)V_{BS}/V_T} \tag{3.13}$$

The sine MOS translinear circuit is shown in Fig. 3.9.

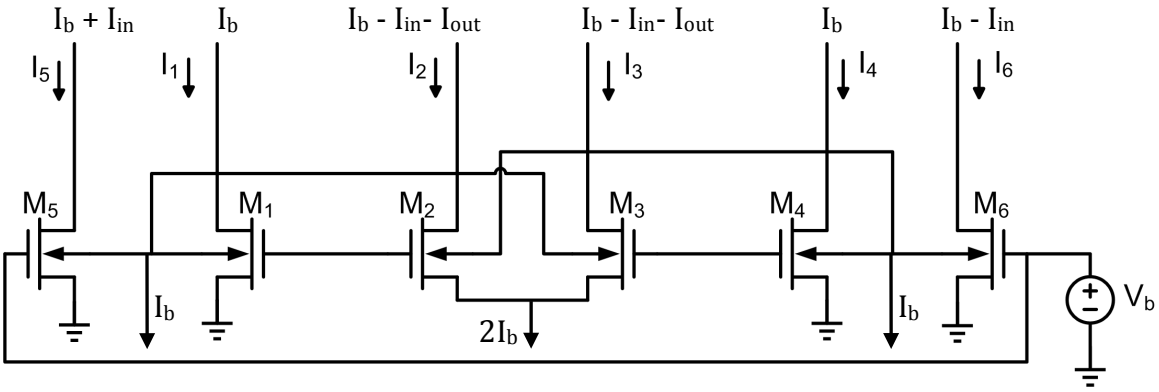

Fig. 3.9 Circuit realizing equation structure (3.57)

In Fig. 3.9, the currents I_1 to I_6 are the drain currents of the MOS transistor M_1 to M_6 respectively. For the drain currents of M_1, M_2, M_3, and M_4, we have

$$\frac{I_1 I_3}{I_2 I_4} = e^{\frac{\kappa}{V_T}(V_{GS1}-V_{GS2}+V_{GS3}-V_{GS4})+\frac{1-k}{V_T}(V_{BS1}-V_{BS2}+V_{BS3}-V_{BS4})} \tag{3.41}$$

Since the gates of M_1 and M_2 are connected and the gates of M_3 and M_4 are connected together as well, we have

$$V_{G1} = V_{G2}\,, V_{G3} = V_{G4} \tag{3.42}$$

Because the sources of M_1 and M_4 are grounded and the sources of M_2 and M_3 are connected, we have

$$V_{S1} = V_{S4}\,, V_{S2} = V_{S3} \tag{3.43}$$

From Equation (3.42) and (3.43), we have

$$V_{GS1} - V_{GS2} + V_{GS3} - V_{GS4} = 0$$

and now the Equation (3.41) becomes

$$\frac{I_1 I_3}{I_2 I_4} = e^{\frac{1-k}{V_T}(V_{BS1}-V_{BS2}+V_{BS3}-V_{BS4})} \tag{3.44}$$

Similarly, from Equation (3.43), the source voltage terms cancel out, and we have

$$\frac{I_1 I_3}{I_2 I_4} = e^{\frac{1-k}{V_T}(V_{B1}-V_{B2}+V_{B3}-V_{B4})} \tag{3.45}$$

For the drain currents of MOS transistor M_5 and M_6, we have

$$\frac{I_5^2}{I_6^2} = e^{\frac{k}{V_T}(2V_{GS5}-2V_{GS6})+\frac{1-k}{V_T}(2V_{BS5}-2V_{BS6})} \tag{3.46}$$

And since the gates of M_5 and M_6 are connected together and the sources of M_5 and M_6 are both grounded, we have

$$V_{G5} = V_{G6}\,, V_{S5} = V_{S6}\,, V_{GS5} = V_{GS6} \tag{3.47}$$

And therefore, Equation (3.46) becomes

$$\frac{I_5^2}{I_6^2} = e^{\frac{1-k}{V_T}(2V_{B5}-2V_{B6})} \tag{3.48}$$

From Fig. 3.9, we see that the back gates of M_1, M_5, and M_3 are connected together as well as the back gates of M_2, M_6, and M_4. So we have

$$V_{B1} = V_{B5} = V_{B3}\,, V_{B2} = V_{B6} = V_{B4} \tag{3.49}$$

And the Equation (3.45) can be written as:

$$\frac{I_1 I_3}{I_2 I_4} = e^{\frac{1-k}{V_T}(V_{B5}-V_{B6}+V_{B5}-V_{B6})} \tag{3.50}$$

From Equation (3.48) and Equation (3.50), we have

$$\frac{I_1 I_3}{I_2 I_4} = \frac{I_5^2}{I_6^2} \tag{3.51}$$

Let's set the drain currents of the six MOS transistors to these values

$$I_2 = I_b - I_{in} - I_{out} \tag{3.52a}$$

$$I_3 = I_b + I_{in} + I_{out} \tag{3.52b}$$

$$I_5 = I_b + I_{in} \tag{3.52c}$$

$$I_6 = I_b - I_{in} \tag{3.52d}$$

$$I_1 = I_4 = I_b \tag{3.52e}$$

Where the I_{in} is the input current, Iout is the output current, and I_b is the bias current. So the output current becomes

$$I_{out} = \frac{1}{2}(I_3 - I_2 - 2I_{in}) \tag{3.53}$$

If we plug the drain current expressions (3.52a)-(3.52e) to left-hand side and right-hand side of Equation (3.51), then we have

$$\frac{I_1 I_3}{I_2 I_4} = \frac{I_b(I_b + I_{out} + I_{in})}{(I_b - I_{out} - I_{in})I_b} = \frac{1 + \frac{I_{out}}{I_b} + \frac{I_{in}}{I_b}}{1 - \frac{I_{out}}{I_b} - \frac{I_{in}}{I_b}} \tag{3.54}$$

and

$$\frac{I_5^2}{I_6^2} = \frac{(I_b + I_{in})^2}{(I_b - I_{in})^2} = \frac{(1 + \frac{I_{in}}{I_b})^2}{(1 - \frac{I_{in}}{I_b})^2} \tag{3.54}$$

From Equation (3.51), the right hand sides of Equation (3.54) and Equation (3.55) are equal to each other, so we get

$$\frac{1 + \frac{I_{out}}{I_b} + \frac{I_{in}}{I_b}}{1 - \frac{I_{out}}{I_b} - \frac{I_{in}}{I_b}} = \frac{(1 + \frac{I_{in}}{I_b})^2}{(1 - \frac{I_{in}}{I_b})^2} \tag{3.56}$$

If we normalize the input and out put current as follows:

$$y = \frac{I_{out}}{I_b}, x = \frac{I_{in}}{I_b} \tag{3.57}$$

Then the Equation (3.57) becomes:

$$\frac{1+y+x}{1-y-x} = \frac{(1+x)^2}{(1-x)^2} \tag{3.58}$$

By simplifying the Equation (3.58), it can be equated to

$$y = \frac{x - x^3}{1 + x^2} \tag{3.59}$$

Since the sine function can be approximated by a rational function [5]

$$0.3\sin \pi x \approx \frac{x - x^3}{1 + x^2} \tag{3.60}$$

So from Equation (3.59) and Equation (3.60), we have

$$y \approx 0.3\sin \pi x \tag{3.61}$$

And therefore the normalized output current is the sine function of the normalized input current:

$$\frac{I_{out}}{I_b} \approx 0.3 \sin \pi(\frac{I_{in}}{I_b}) \tag{3.62}$$

The plots of the sine function (3.61) and the rational approximation of the sine function (3.59) are shown in the Fig. 3.10 and Fig. 3.11 over |x|<5 and |x|<1, respectively. From Fig. 3.10, we can see that the equation (3.59) only fits to the sine function (3.61) when x is ranging from -1 to 1. However, when x is within the [-1, 1] range, the rational approximation function (3.59) fits to the sine function (3.61) very well. Therefore, if the drain currents of circuit in Fig. 3.9 satisfy the equation (3.52a)-(3.52e), then when the input current I_{in} is ranging from $-I_b$ to I_b, the output current I_{out} has the shape of the sine wave.

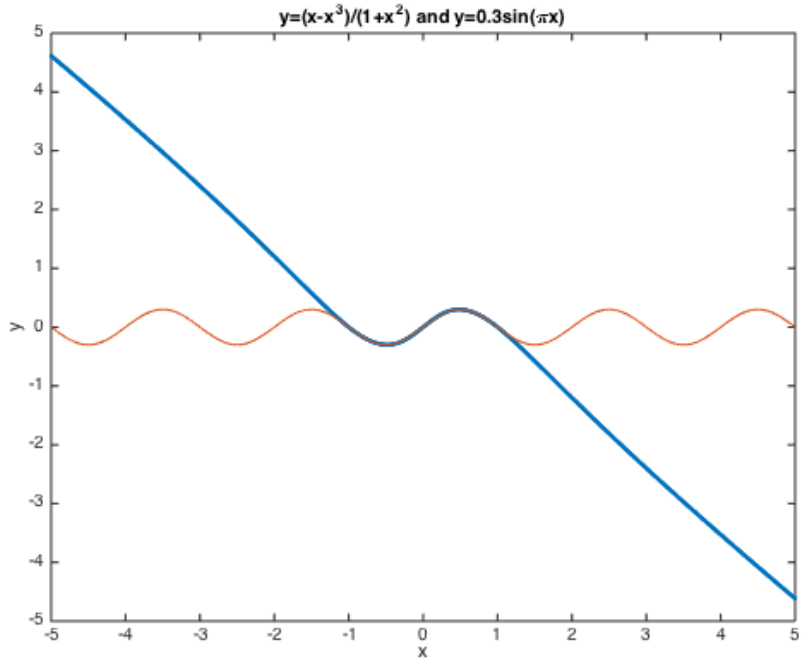

Fig. 3.10 Matlab plots of function $y = \frac{x-x^3}{1+x^2}$ and $y = 0.3\sin(\pi x)$ when -5 < x < 5

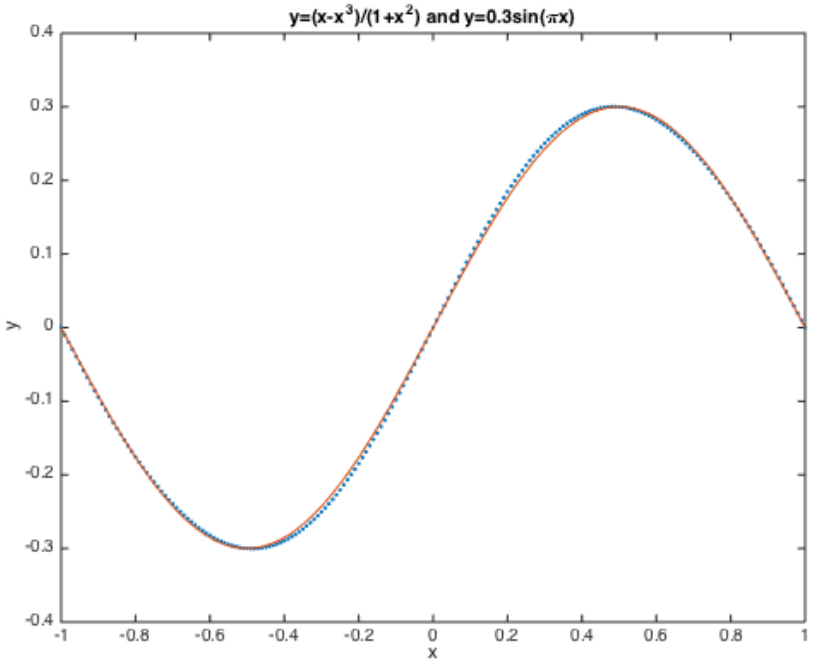

Fig. 3.11 Matlab plots of function $y = \frac{x-x^3}{1+x^2}$ and $y = 0.3\sin(\pi x)$ when -1 < x < 1

3.3 Simulations of MOS Translinear sin(x)-Circuits

Mulder et.al. have built a breadboard version of the sine translinear circuit and experimentally verified the theory [5]. However, due to the breadboard realization, the mismatch in their results is quite large. To verify the derivation above, I created the circuit shown in Fig. 3.12 and the completely designed version in Fig. 3.13 using PSpice and ran simulation on this ideal sine translinear MOS circuit. The values of the currents, voltages, and W/L ratios of the MOS transistors in Fig. 3.12 and Fig. 3.13 are discussed in detail in section 3.3.1 and section 3.3.2.

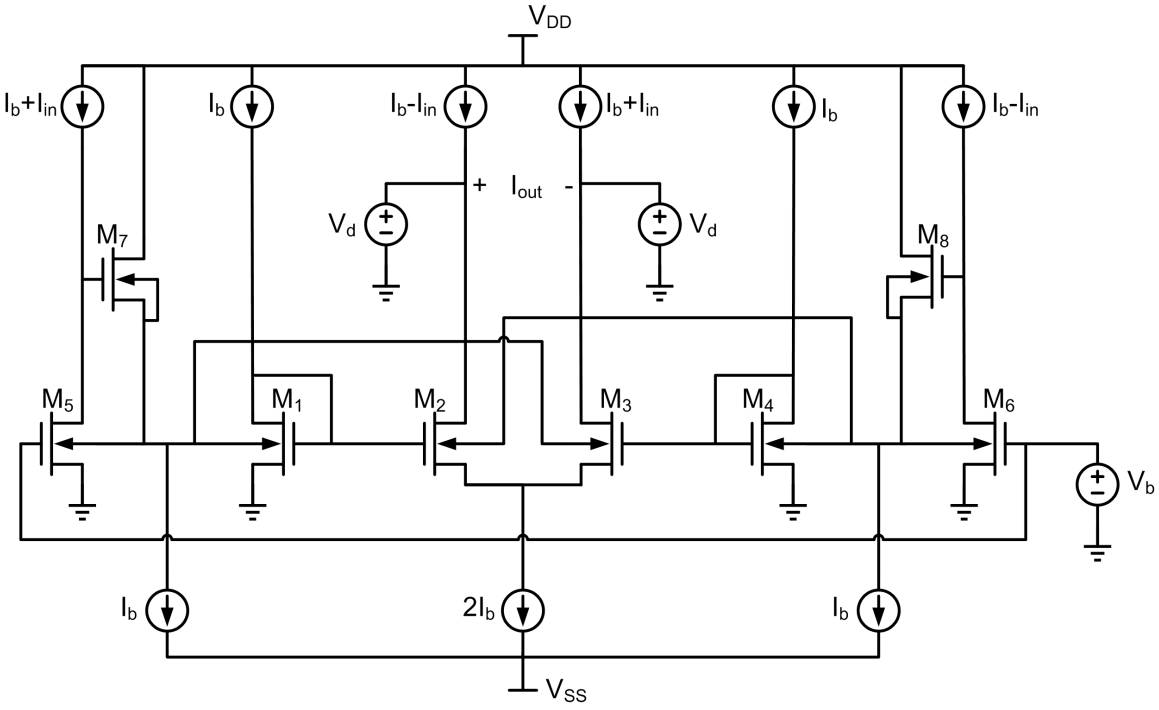

Fig. 3.12 Ideal MOS translinear circuit realizing sine-approximation function

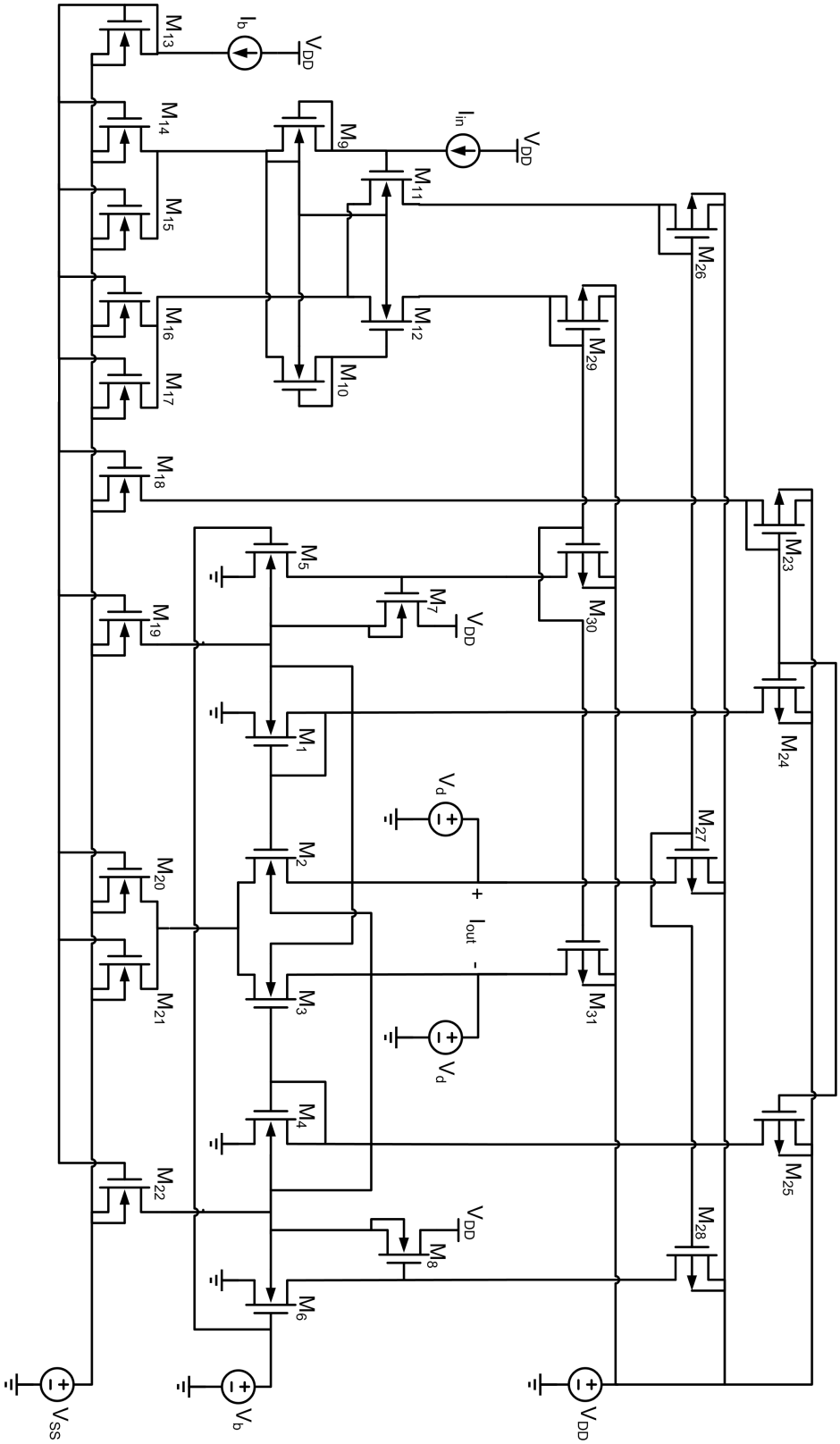

Fig. 3.13 MOS translinear circuit realizing sine-approximation function

From the derivation above, we know that to generate the sine output current, two conditions should be satisfied. The first condition is that all the MOS transistors should work in the region where Equation (3.13) holds. Therefore, all the MOS transistors should work in the saturation region and subthreshold region. So, we should set

$$V_{DS} > V_{GS} - V_{th}, \text{and } V_{GS} < V_{th} \tag{3.63}$$

for all MOS transistors. However, we still need to satisfy Equation (3.12), i.e.

$$V_{DS} > 4U_T \tag{3.12}$$

for all transistors to neglect the V_{DS} in Equation (3.11) in order to get Equation (3.13). The second condition is that the drain currents of the six MOS transistors have to satisfy the relationship in Equation (3.52a) – (3.52e) to get the rational sine approximation function (3.59) between the input and output currents. Also note that this approximation is only valid when the input current is within the range [$-I_b$, I_b].

3.3.1 Ideal Model

To satisfy the two conditions in the simulation, the current sources with the desired values in Equation (3.52a)-(3.52e) are used to supply currents of the MOS transistors. The two MOS transistors M_7 and M_8 are used to keep M_5 and M_6 in saturation [5] and the two voltage sources at the drains of M_2 and M_3 are used to keep $V_{DS} > 4U_T$ [13].

The ideal translinear sine circuit is depicted in Fig. 3.12. The supply voltages V_{DD} and V_{SS} are +1 V and -1 V respectively. The bias voltage V_b at the gates of M_5 and M_6 is 350 mV. The two voltage sources at the drains of M_2 and M_3 are set to 500 mV. The bias current I_b is 4 nA and therefore the input current I_{in} is set to vary from -4 nA to 4 nA. The output current I_{out} is the current in the voltage source V_d at the drains of M_2 and M_3. The

model of the MOS transistor used in this simulation is mnmosis in the bicmos12 library and we set W/L = 108u/7u. We define the input current Iin as a global parameter and use the linear DC sweep to let it vary from -4.5 nA to 4.5 nA with the increment of 0.001nA. The simulation results of the output current are shown in Fig. 3.14. The black line is the current in the voltage source at the drain of M_2, which equals to the output current I_{out} and the red line represent the current in the voltage source at the drain of M_3, which is the negative of the output current. We can see that the absolute values of the two currents are equal and they have the shape similar to the sine wave. Also, the peaks of the curves are around the theory value $0.3I_b$, which is 1.2 nA. Therefore, we can say that the simulation results match the theory very well.

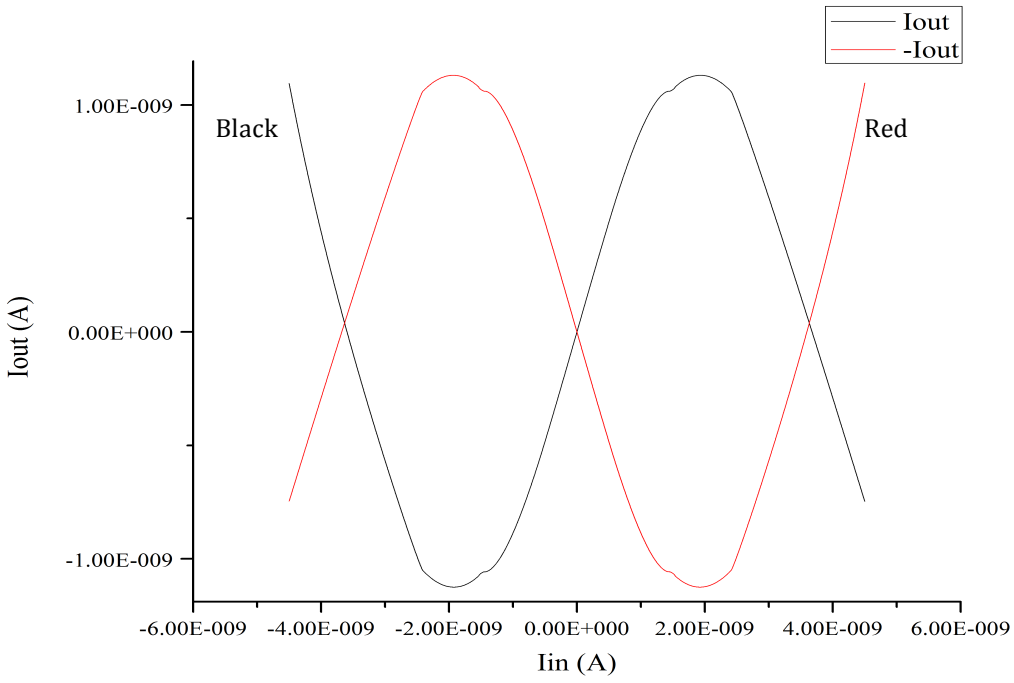

Fig. 3.14 Output currents of the Ideal MOS translinear sin(x)-circuit

3.3.2 Realistic Model

To simulate a more realistic model, we substitute the current sources to current mirrors to supply the currents of the translinear sine circuit and the new circuit is shown in Fig. 3.13. The supply voltages V_{DD} and V_{SS} are +1 V and -1 V respectively. The bias voltage V_b is 350 mV and the two voltage sources at the drains of M_2 and M_3 are 500 mV. The bias current I_b is still 4 nA. However, we set the input current I_{in} to vary from -1 nA to 10 nA with the increment of 0.001nA due to the phase shift of the output current in this sine circuit. And now Iin is not a global parameter but just a current source and we still use the linear DC sweep for this simulation. The model of the nMOS transistors is mnmosis in the bicmos12 library with W/L ratio of 108u/7u and the model of pMOS transistors is mpmosis in the same library.

In Fig. 3.15, the output currents I_{out} and - I_{out} in the voltage sources at the drains of M_2 and M_3 are depicted in black and red lines respectively. Similar to the simulation results of the ideal translinear sine circuit, the two currents are of the sine-like shape and their peak values are around the theory value $0.3I_b$ (=1.2 nA). However, there is a phase shift in this simulation. This phase shift results from the fact that the drain currents do not exactly satisfy the Equation (3.52a)-(3.52e). And the little distortion in the output current plot seems to result from the saturation of some MOS transistors.

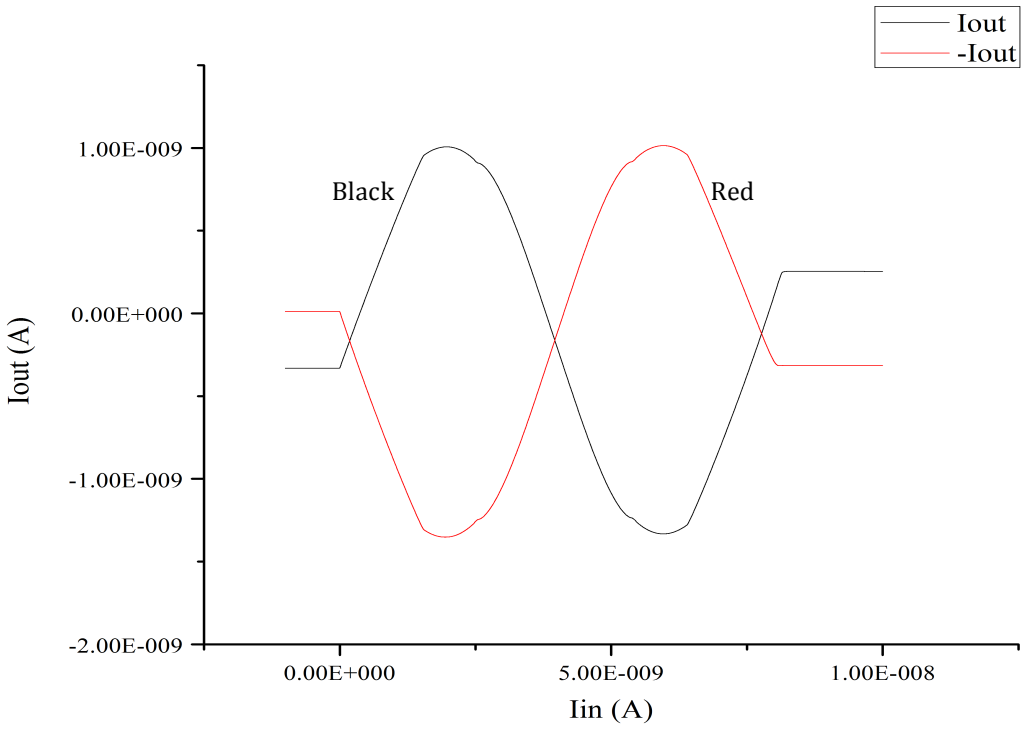

Fig. 3.15 Output currents of the MOS translinear sin(x)-circuit

3.4 Creation of Sine-Gordon Lattice Circuit

Since the third sine-Gordon lattice system that realizes the sine-lattice equation gives the best simulation results, we will create the circuit for the basic cell of this system. However, there are three sine functions in each cell of this system, so we will use the 2-sine cell structure shown in Fig. 2.26 instead of the 3-sine cell structure used in the simulation.

For the two sine functions in this sine-Gordon cell, we use Mulder's MOS translinear sin(x)-circuit shown in Fig. 3.13, which gives a good approximation of the sine function within the $[-\pi, \pi]$ range. We could use the current mirrors to realize the current adder and subtractor; a current subtractor is shown in Fig. 3.16.

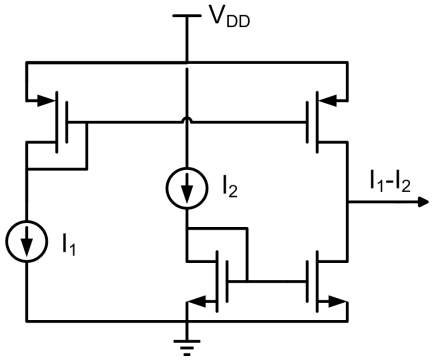

Fig. 3.16 Current subtractor

For each of the two integrators, we use a capacitor and an operational transconductance amplifier as the current integrator. The equation for this current integrator is

$$I_{out} = g_m v_i = g_m \int_0^t \frac{1}{C} I_{in} \mathrm{d}\tau + g_m v(0) \tag{3.64}$$

and the current integrator is shown in Fig. 3.17. By connecting these functional circuits together using the method in Fig. 2.26, the complete circuit for a sine-Gordon cell is obtained and depicted in Fig. 3.18, where W/L = 108u/7u for all 101 MOS transistors.

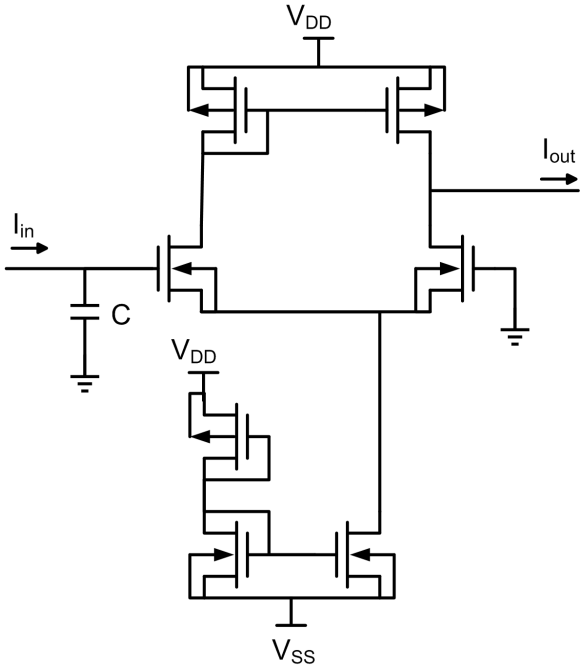

Fig. 3.17 Integrator circuit

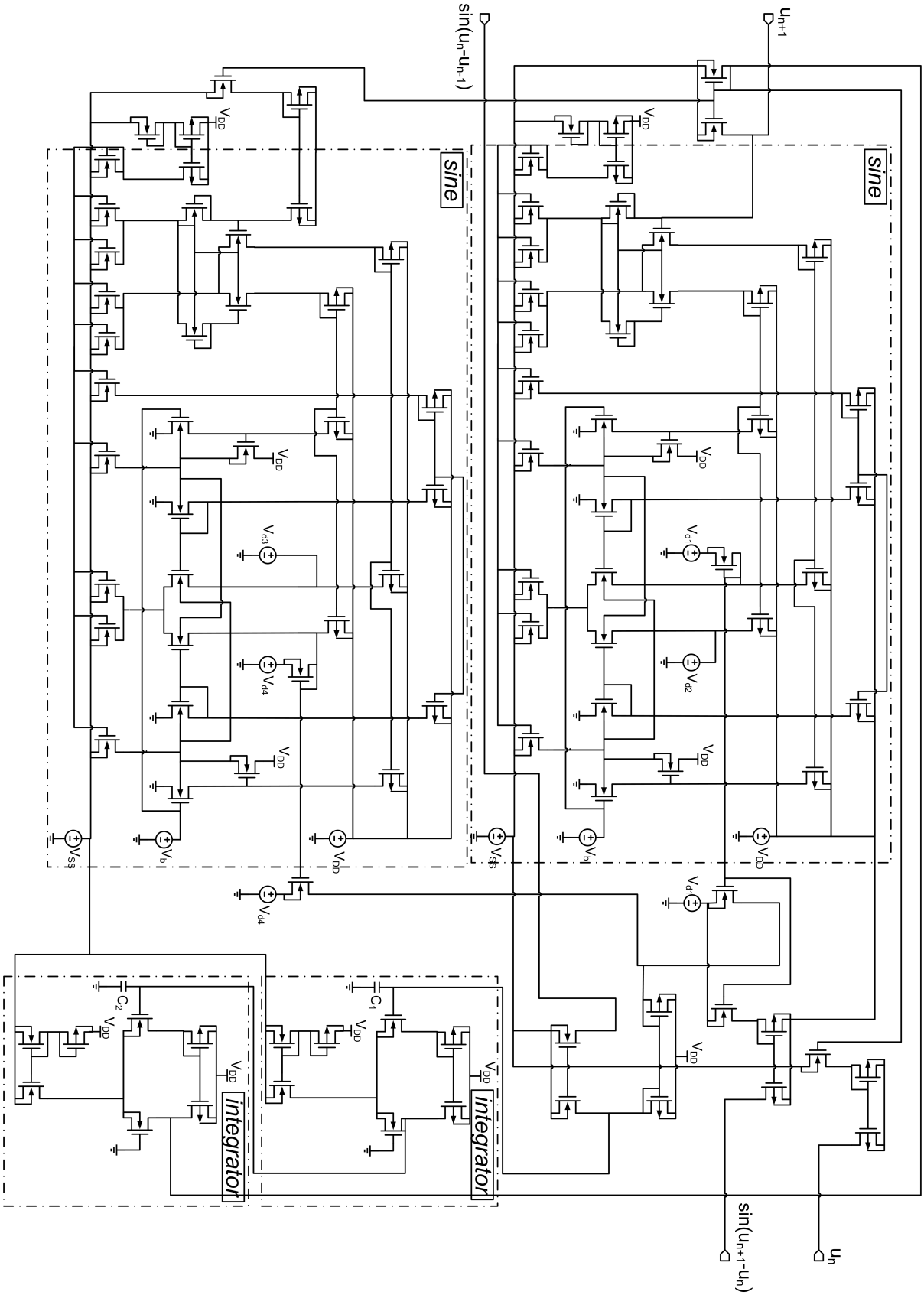

Fig. 3.18 Complete circuit for the nth cell of the third sine-Gordon lattice system

3.5 Conclusions

Two MOS translinear circuits realizing sin(x) approximation function have been simulated using PSpice. Both simulation results showed that the differential output current is approximately the sine function of the input current when the input is within the range [-bias current, bias current]. The input current, bias current and voltages sources in this design are all very low, and therefore we use this sin(x)-circuit to create the circuit for the cell of the sine-Gordon lattice system that realize the sine-lattice equation. We also use the current mirrors for current addition and subtraction, and capacitor and operational transconductance amplifier as integrator circuits to construct this sine-Gordon cell. The complete sine-Gordon cell circuit contains 101 MOS transistors and 2 capacitors.

Chapter 4 Conclusions

4.1 Summary

In chapter 2, we introduced three forms of sine-Gordon equation, namely conventional discrete sine-Gordon equation, Orfanidis's discrete sine-Gordon equation, and sine-lattice equation. We also discussed the solutions for each discrete sine-Gordon equation and made plots of these solutions or the differences between solutions of adjacent modes. Then, based on the three discrete equations, we used Matlab Simulink to create the nth cell of the sine-Gordon lattice systems and then connected the cells together to obtain the entire lattice system. The inputs of the sine-Gordon lattice systems are the exact solutions of each discrete equation. From the plots of the discrete sine-Gordon equation solutions, we take the difference between the adjacent outputs as the transmitting signal. The simulation results are presented by the Amplitude versus Time plots of the outputs of basic cells and the outputs of the subtractors, i.e. the transmitting signals. The simulation results show that all three systems could propagate the bell-shaped signal constantly without too much amplitude loss and distortion and the third system gives the best results. And therefore, we prefer to use the sine-lattice equation to construct the sine-Gordon lattice system. And for the third lattice system, another method to create the basic cell was also discussed in order to decrease the number of the sine functions in the lattice system.

In chapter 3, first, a brief review of translinear circuits and translinear principle was given with some simple examples. Next, we introduced the translinear principle for MOS translinear circuits and discussed the MOS translinear circuits utilizing back gates. We also gave some examples of the MOS translinear circuits. Several bipolar or MOS

translinear circuits that realize the sine function were introduced. In the next part, we mainly discussed a MOS translinear sin(x)-circuit in Mulder's paper [5]. First, we presented the principle of operation of this sin(x)-circuit with derivation and plots. Then we used PSpice to create and simulate the ideal and realistic models of this circuit. The simulation results of two MOS translinear circuits realizing sin(x) approximation function were shown to result by the output current verses input current plots and it was shown that the differential output current is approximately the sine function of the input current when the input is ranging from negative bias current to positive bias current. The input current, bias current and voltages sources in this design are all very low, and therefore this sin(x)-circuit structure is suitable for realizing the sine functions in our Sine-Gordon lattice circuit. Then we used the MOS translinear circuit above to create the 2-sine basic cell of the third sine-Gordon system in chapter 2 since this system gives the best simulation results. The complete circuit that contains two MOS translinear sin(x)-circuitsis, two operational transconductance amplifier integrator circuits, and several current mirrors for current addition and subtraction was presented in Fig. 1.18 and it contains 101 MOS transistors and 2 capacitors for each cell.

4.2 Future Directions

For the three sine-Gordon lattice systems in chapter 2, we can try different forms of the inputs, change the initial conditions of the integrators, vary the amplitude, phase, frequency, and bias of the sine functions, and alter the structure of the nth cells to obtain better results. Other discrete forms of the sine-Gordon equation could be utilized to create the nth cell in the system as well. Besides the sine-Gordon equation, we could discretize

the sinh-Gordon equation and create the sinh-Gordon lattice system using the similar methods.

For the sin(x)-Circuit part, we could try other MOS transistor models, for example, the 0.35u MOS transistor, which is much more appropriate in term of application, or make some changes to the MOS translinear circuits to get better sine-shaped outputs. We could create the sin(x)-circuits based on other sine approximation methods. Besides utilizing the bulk voltages of MOS transistor under weak inversion, we could use the front gate voltages as well. Also, there are many other sine circuits that consist of bipolar transistors that might be suitable for our sine-Gordon lattice system as well.

Another open problem about the MOS translinear sin(x)-circuit is that besides the bias voltage at the gate, we still have two bias voltages at the drains of two MOS transistor to keep them in weak inversion and output the sine current. So, in future works, we should try to use only one bias voltage in the entire sin(x)-circuit.

Besides the creation of the sine-Gordon lattice system and the sin(x)-circuit, we could also research on the proper circuits to realize the integrators, adders, subtractors, and amplifiers in the sine-Gordon lattice system to obtain better performance of the cell circuit when transmitting soliton signals.

After that, we could connect the circuits for sine-Gordon cell together to obtain the complete circuit for sine-Gordon lattice system and simulate this complete circuit for the solition transmission.

In Hirota's paper [21], an exact solution of sine-Gordon for the case of multiple-soliton propagation was obtained. We could use the n-soliton solution as the input of our sine-Gordon lattice system for multiple-soliton transmission.

Reference

[1] Russell, J. S. (1844, September). Report on waves. In *14th meeting of the British Association for the Advancement of Science* (Vol. 311, p. 390).

[2] Korteweg, D. J., & De Vries, G. (1895). Xli. on the change of form of long waves advancing in a rectangular canal, and on a new type of long stationary waves.*The London, Edinburgh, and Dublin Philosophical Magazine and Journal of Science*, *39*(240), 422-443.

[3] Scott, A. C., Chu, F. Y. F., & McLaughlin, D. W. (1973). The soliton: A new concept in applied science. *Proceedings of the IEEE*, *61*(10), 1443-1483.

[4] Ivancevic, V., & Ivancevic, T. (2013). Sine-Gordon solitons, kinks and breathers as physical models of nonlinear excitations in living cellular structures. *arXiv preprint arXiv:1305.0613.*

[5] Mulder, J., van der Woerd, A., Serdijin, W., & van Roermund, A. (1995). Application of the Back Gate in MOS Weak Inversion Translinear Circuit. *IEEE Transactions on Circuits and Systems I: Fundamental Theory and Applications , 42(11)*, 958-962.

[6] Dai, C. Q., Cen, X., & Wu, S. S. (2009). Exact Travelling Solutions of Discrete sine-Gordon Equation via Extended Tanh-Function Approach. *Nonlinear Analysis , 70*, 58-63.

[7] Cisneros, L., & Minzoni, A. (2008). Asymptotics for kink propagation in the discrete Sine-Gordon equation. *Physica D: Nonlinear Phenomena , 237(1)*, 50-65.

[8] Orfanidis, S. (1978). Discrete sine-Gordon equations. *Physical Review D , 18(10)*, 3822.

[9] Dai, C. Q., Yang, Q., & Zhang, J. F. (2004). New Exact Travelling Wave Solutions of the Discrete Sine-Gordon Equation. *Z. Naturforsch , 59a*, 635-639.

[10] Takeno, S., & Homma, S. (1986). A Sine-Lattice (Sine-Form Discrete Sine-Gordon) Equation–One-and Two-Kink Solutions and Physical Models–. *Journal of the Physical Society of Japan , 55(1)*, 65-75.

[11] Gilbert, B. (1975). Translinear circuits: A proposed classification. *Electronics Letters , 11(1)*, 14-16.

[12] Gilbert, B. (1996). Translinear circuits: an historical overview. *Analog Integrated Circuits and Signal Processing , 9(2)*, 95-118.

[13] Andreou, A. G., & Boahen, K. A. (1996). Translinear circuits in subthreshold MOS. *Analog Integrated Circuits and Signal Processing , 9(2)*, 141-166.

[14] Serrano-Gotarredona, T., Linares-Barranco, B., & Andreou, A. G. (1999). A general translinear principle for subthreshold MOS transistors. *Circuits and Systems I: Fundamental Theory and Applications, IEEE Transactions on , 46(5)*, 607-616.

[15] Gray, P. R., Hurst, P. J., Lewis, S. H., & Meyer, R. G. (2001). *Analysis and Design of Analog Integrated Circuits* (Fourth ed.). New York: Wiley.

[16] Mulder, J., van Der Woerd, A. C., Serdijn, W. A., & Van Roermund, A. H. (1995). Translinear sin (x)-circuit in MOS technology using the back gate. *Solid-State Circuits Conference, 1995. ESSCIRC '95. Twenty-first European* , 82-85.

[17] Greeneich, E. (2012). *Analog Integrated Circuits.* Springer US.

[18] Gilbert, B. (1977). Circuits for the precise synthesis of the sine function. *Electronics Letters , 13(17)*, 506-508.

[19] Gilbert, B. (1982). A monolithic microsystem for analog synthesis of trigonometric functions and their inverses. *IEEE Journal of Solid-State Circuits , 17(6)*, 1179-1191.

[20] Fried, R., & Enz, C. (1996). MOST implementation of Gilbert sin (x) shaper. *Electronics Letters , 32(22)*, 2073-2074.

[21] Hirota, R. (1972). Exact solution of the sine-Gordon equation for multiple collisions of solitons. *Journal of the Physical Society of Japan*, *33*(5), 1459-1463.